NEAR REPORT TR 2

July 25, 1967

CALCULATION OF LAMINAR BOUNDARY LAYER-SHOCK WAVE INTERACTION ON COOLED WALLS BY THE METHOD OF INTEGRAL RELATIONS

by

Frederick K. Goodwin
Jack N. Nielsen
Larry L. Lynes

prepared for

Ames Research Center
National Aeronautics and Space Administration

Contract No. NAS2-4216
NEAR Project 116/C

Nielsen Engineering & Research, Inc.
850 Maude Ave., Mountain View, Calif. 94040
Telephone (415) 968-9457

TABLE OF CONTENTS

LIST OF SYMBOLS

a	local speed of sound
a_o	speed of sound at outer edge of boundary layer at x_o
a_1	speed of sound at outer edge of boundary layer for any value of x
c_p	specific heat of gas at constant pressure
c_o, c_1, c_2, c_3	coefficients specifying the velocity profile of the outer flow, Equation (40)
$\dot{c}_o, \dot{c}_1, \dot{c}_2, \dot{c}_3$	derivatives of velocity profile coefficients with respect to ξ
C	numerical constant in viscosity relationship, $\mu/\mu_o = CT/T_o$
C_f	skin-friction coefficient, $\tau_w/(1/2)\rho_1 u_1^2$
d_n	defined by Equation (A-7)
E_o	coefficient specifying the temperature profile of the outer flow, Equations (41) or (42)
$\dot{E}_o$	derivative of temperature profile coefficient with respect to ξ
$\overline{f}_n$	defined by Equation (A-8)
F_n	defined by Equation (99)
$\dot{g}_n$	dg_n/dc_3, family of definite integrals given by Equation (A-10)
$g_n(c_3)$	family of definite integrals given by Equation (A-9)
$\overline{H}_n$	defined by Equation (A-11)
$\tilde{H}_n$	defined by Equation (B-10)
k	thermal conductivity of gas
ℓ	reference length, taken equal to x_o

m_o	$\left(\frac{\gamma - 1}{2}\right) M_o^2$
m_1	$\left(\frac{\gamma - 1}{2}\right) M_1^2$
M	local Mach number
M_o	Mach number parallel to δ^* line at x_o
M_1	Mach number parallel to δ^* line for any value of x
M_4	value of M_1 at $x = x_i$ just behind shock wave
M_∞	free-stream Mach number
n	index
$\overline{N}_n$	defined by Equation (A-12)
p	local static pressure
p_n, n=2,3,···8	defined by Equations (A-13)
p_t	local stagnation pressure
p_o	static pressure at x_o
p_1	static pressure at edge of boundary layer for any value of x
P_n	family of definite integrals defined by Equation (A-14)
Pr	Prandtl number
q	local heat-transfer rate at the wall
q_o	local heat-trasnfer rate at the wall at $x = x_o$
q_1	local heat-transfer rate at the wall for any value of x
Q_n	family of definite integrals defined by Equation (A-15)

R_o	Reynolds number, $u_o \ell / \nu_o$
R_x	local Reynolds number, $u_1 x / \nu_1$
$s(x)$	y-coordinate of $u = 0$ line between separation and reattachment
S	temperature parameter, $S = \frac{T_t}{T t_o} - 1$
$S_i(y)$	initial temperature profile at x_o
$S_i(Y)$	initial temperature profile at X_o in Stewartson plane
$S_i(\eta)$	initial temperature profile at ξ_o in Dorodnitsyn plane
S_s	value of S along the $\bar{u} = 0$ line
St	Stanton number
St_o	Stanton number at $x = x_o$
S_w	value of S at the wall, $S_w = \frac{T_w}{T t_o} - 1$
T	local absolute temperature
T_t	local stagnation temperature
T_{t_o}	stagnation temperature at edge of boundary layer at x_o
T_w	temperature of the wall
T_o	temperature at edge of boundary layer at x_o
T_1	temperature at edge of boundary layer at any value of x
u	axial velocity in x,y plane
$\bar{u}$	U/U_1

$u_i(y)$ initial velocity profile at x_o

$\bar{u}_i(\eta)$ initial velocity profile at ξ_o in Dorodnitsyn plane

$\bar{u}_s$ symbol used to represent u component of velocity at the boundary between the inner and outer flow regions; it is always zero, but the symbol is used for clarity

u_o value of u at edge of boundary layer at x_o

u_1 value of u at edge of boundary layer for any value of x

U axial velocity in X,Y plane, ua_o/a_1

$U_i(Y)$ initial velocity profile at X_o in the stewartson plane

U_o value of U at edge of boundary layer at X_o

U_1 value of U at edge of boundary layer for any X

$\dot{U}_1$ $dU_1/d\xi$

v normal velocity in x,y plane

$\bar{v}$ normal velocity in ξ,η plane, $\frac{V}{U_1}\sqrt{\frac{U_o \ell}{\nu_o}}$

v_s value of v at s(x)

$\bar{v}_s$ value of $\bar{v}$ at η_s

v_1 value of v at the edge of boundary layer for any x

V normal velocity in X,Y plane

V_s value of V at Y_s

$\bar{w}$ $\bar{v} + \bar{u}\eta \frac{\dot{U}_1}{U_1}$

$\bar{w}_s$ value of $\bar{w}$ at η_s

x_i value of x at shock wave impingement point

x_r value of x at the reattachment point

x_s value of x at the separation point

x,y coordinates of two-dimensional flow under consideration

x_o value of x where separation interaction begins

X,Y coordinates after Stewartson transformation;

$$X = \int_o^x \frac{p_1 a_1}{p_o a_o}\, dx \; ; \quad Y = \int_o^y \frac{\rho_1 a_1}{\rho_o a_o}\, \frac{\rho}{\rho_1}\, dy$$

X_o value of X corresponding to x_o

Y_s value of Y corresponding to $s(x)$

α_g angle of wedge generating shock wave

α_s value of $\partial\bar{u}/\partial\eta$ at η_s

γ ratio of specific heats

δ boundary-layer thickness

δ^* displacement thickness in physical plane

δ^{**} momentum thickness in physical plane

δ_i^* displacement thickness of inner flow

δ_o^* displacement thickness of outer flow

$\eta_s(\xi)$ η-coordinate of the $\bar{u} = 0$ line between separation and reattachment

$\dot{\eta}_s$ derivative of η_s with respect to ξ

μ absolute viscosity

μ_o absolute viscosity at outer edge of boundary layer at x_o

ν	kinematic viscosity, μ/ρ
ν_o	kinematic viscosity at outer edge of boundary layer at x_o, μ_o/ρ_o
ν_1	value of ν at edge of boundary layer for any x
ξ_o	value of ξ corresponding to x_o
ξ, η	coordinates in Dorodnitsyn plane, $\xi = \int_0^X \frac{U_1}{U_o} \frac{dX}{\ell}$, $\eta = \frac{U_1}{U_o \ell} \sqrt{\frac{U_o \ell}{\nu_o}}\, Y$
ρ	local mass density
ρ_o	value of ρ at edge of boundary layer at x_o
ρ_1	value of ρ at edge of boundary layer for any x
τ_w	shear stress at the wall
ϕ	slope of streamline outside of boundary layer
ϕ_c	integration constant defined by Equations (68) or (69)
ϕ_o	value of ϕ at $x = x_o$
ϕ_1	value of ϕ for any x
ϕ_4	value of ϕ_1 at $x = x_i$ just behind shock wave
Ψ	mass flow in the boundary layer
$\overline{\Psi}$	mass flow in the boundary layer in Dorodnitsyn plane

CALCULATION OF LAMINAR BOUNDARY LAYER-SHOCK WAVE INTERACTION ON COOLED WALLS BY THE METHOD OF INTEGRAL RELATIONS

By Frederick K. Goodwin, Jack N. Nielsen
and Larry L. Lynes
Nielsen Engineering & Research, Inc.

SUMMARY

The present report is an informal report submitted to Ames Research Center, NASA, in accordance with the reporting requirements of NASA Contract NAS2-4216. A complete description is given of the mathematical analysis of the problem. This analysis is based on the method of integral relations as developed in previous work by the present authors and extended to the highly-cooled wall case under an existing contract with the Air Force Flight Dynamics Laboratory, Contract No. F33615-67-C-1096. It is noteworthy that a criterion has been developed to determine the unique solution to the interaction problem for a given case. Based on the analysis, a computer program has been developed to perform the calculations. A complete description of the input requirements of the program is included. A form to be used for preparing input data is included. Comparisons are made between calculated pressure distributions, velocity profiles, and skin-friction coefficients and those obtained experimentally.

INTRODUCTION

In the design of inlets for air-breathing propulsion systems it is important that account be taken of the interaction between any shock waves and the boundary layer. It is the purpose of the present report to describe an extension of the methods developed in References 1 and 2 to the problem of laminar boundary layer-shock wave interaction for highly cooled walls. In the above references a method was developed for the calculation of laminar separation with free interaction by the method of integral relations for a two-dimensional flat plate followed by a wedge, and a circular cylinder followed by an axisymmetric flare. The work to be described in this report relies heavily on work presently being done for the Air Force Flight Dynamics Laboratory of Wright-Patterson Air Force Base under Contract No. F33615-67-C-1096. This contract extends the work of Reference 2 to second-order coupling between temperature and velocity profiles. Such coupling must be taken into account for accurate pressure distributions on highly cooled walls. It is also necessary if realistic heat-transfer results are to be obtained.

In References 1 and 2, it was found possible to calculate a separated flow for a given configuration for each assumed location of the beginning of interaction over a wide range of such locations. However, no uniqueness condition was developed to determine the position of the separation point to be expected in practice. In the present investigation, it was possible to extend the calculative method downstream of the reattachment point and to develop a uniqueness criterion based on the calculated behavior of the solutions in this region. The criterion is simply that the final pressure attains a specified value and that the first and second derivatives of the pressure with respect to downstream distance both be zero where this specified value is attained. This criterion, which arises naturally out of the behavior calculated by the method of

integral relations, is the same as that recently found by Reyhner and Flügge-Lotz in Reference 3 using finite-difference methods.

In this report the equations which are solved are presented without detailed derivation. The method of treating the flow across the impingement point is described as well as the iteration procedure to determine the unique solution. Comparisons between experiment and theory are made.

GENERAL CONSIDERATIONS

Description of Problem

The problem under consideration is that of calculating laminar boundary-layer flow, either separated or unseparated, on a highly-cooled flat plate resulting from an oblique shock wave incident on the boundary layer. Typical pressure distributions for such an interaction are shown in Figure 1. For the unseparated case (Fig. 1(a)) the entire length of the interaction is assumed to be governed by free interaction between the boundary layer and the supersonic outer flow. By free interaction we mean that the pressure distribution of the outer flow is the result of local mutual interaction between the boundary layer and the outer flow independent of the downstream means initiating the interaction.

For the separated case (Fig. 1(b)), free interaction is assumed to apply from the beginning of the interaction, x_o, to the point where the first plateau pressure is reached ($dp/dx = 0$). From this point to the shock impingement point the boundary condition of constant pressure is imposed. From the shock impingement point on downstream, free interaction is again assumed. The final pressure distribution culminates in a second plateau region.

For both the unseparated and separated cases a downstream pressure boundary condition similar to that used by Reyhner and Flügge-Lotz in Reference 3 arises naturally in the method of integral relations. For a flat plate, if the flow is to make a smooth transition into a constant pressure flow downstream of the impingement point both dp/dx and d^2p/dx^2 must approach zero together. When this condition is specified, a unique solution can be found for given positions of shock impingement and the beginning of interaction. When p as well as dp/dx and d^2p/dx^2 are specified, then a unique position of the beginning of interaction can also be found, and the whole flow becomes unique.

The particular configuration treated in the analysis and the computer program is shown in Figure 2. An oblique shock wave of

known strength strikes the boundary layer on a flat plate at impingement point, x_i. The beginning of the free interaction between the boundary layer and the outer flow occurs at x_o. At this point the Mach number, M_o, the stagnation temperature, T_{t_o}, and the Reynolds number per foot, R_o/x_o, at the edge of the boundary layer are known and the velocity profile is assumed to be of the Blasius type. The flat plate is at uniform arbitrary temperature, T_w. The interaction causes the boundary layer to thicken and to separate at x_s. The boundary layer continues to thicken until the impingement point, x_i, is reached. At this point the rate of change of the displacement thickness with x, $d\delta^*/dx$, is changed discontinuously so that the boundary layer is turned back toward the plate and reattaches at x_r. From there on the boundary layer continues to thin until $d\delta^*/dx$ is zero.

During the last part of the computation an iterative calculation is made to see if the downstream boundary condition, $dp/dx = d^2p/dx^2 = 0$, can be satisfied. If the initially assumed value of $d\delta^*/dx$ just behind the shock wave is not correct, a new value is chosen and the last part of the computation, from x_i on, is repeated. This iteration procedure, which converges, is described in detail in a later section.

Assumptions

A number of assumptions have been made in the analysis.

(1) The governing equations are those for a compressible laminar boundary layer.

(2) The Prandtl number is unity.

(3) The fluid behaves as an ideal gas with constant specific heats.

(4) The flat plate is at uniform arbitrary temperature.

(5) The viscosity varies linearly with temperature.

(6) The pressure at the outer edge of the boundary layer is governed by the Prandtl-Meyer relationship.

(7) The pressure across the boundary layer is constant.

Partial Differential Equations and Boundary Conditions

The differential equations governing the flow are those for the compressible laminar boundary layer. This compressible flow problem is first reduced to an equivalent incompressible flow problem by the use of the Stewartson transformation. Then a modified form of the Dorodnitsyn transformation, Reference 4, is used to eliminate the viscosity explicitly and normalize the axial velocity component.

Physical plane.- In the physical or compressible plane the laminar boundary-layer equations are, from Reference 5, pp. 379-381,

$$\rho\left(u\frac{\partial u}{\partial x}+v\frac{\partial u}{\partial y}\right)=\rho_1 u_1\frac{\partial u_1}{\partial x}+\frac{\partial}{\partial y}\left(\mu\frac{\partial u}{\partial y}\right) \tag{1}$$

$$\frac{\partial}{\partial x}(\rho u)+\frac{\partial}{\partial y}(\rho v)=0 \tag{2}$$

$$\rho c_p\left(u\frac{\partial T}{\partial x}+v\frac{\partial T}{\partial y}\right)+\rho_1 u u_1\frac{\partial u_1}{\partial x}=\frac{\partial}{\partial y}\left(k\frac{\partial T}{\partial y}\right)+\mu\left(\frac{\partial u}{\partial y}\right)^2 \tag{3}$$

If it is assumed that the Prandtl number is unity and that the specific heat at constant pressure is a constant and if Equation (1) is multiplied by u and added to Equation (3), the energy equation becomes

$$\rho u\frac{\partial T_t}{\partial x}+\rho v\frac{\partial T_t}{\partial y}=\frac{\partial}{\partial y}\left(\mu\frac{\partial T_t}{\partial y}\right) \tag{4}$$

where

$$T_t=T+\frac{u^2}{2c_p} \tag{5}$$

A temperature parameter, S, is defined

$$S = \frac{T_t}{T_{t_o}} - 1 \tag{6}$$

so that Equation (4) becomes

$$\rho u \frac{\partial S}{\partial x} + \rho v \frac{\partial S}{\partial y} = \frac{\partial}{\partial y}\left(\mu \frac{\partial S}{\partial y}\right) \tag{7}$$

The velocity boundary conditions are

$$u = v = 0 \quad \text{at} \quad y = 0 \quad \text{for all} \quad x \tag{8}$$

$$u = u_i(y) \quad \text{at} \quad x = x_o \tag{9}$$

$$\left.\begin{aligned} u &= u_1(x) \\ \frac{\partial u}{\partial y} &= 0 \end{aligned}\right\} \quad \text{at} \quad y = \infty \quad \text{for all} \quad x \tag{10}$$

and the temperature boundary conditions are

$$S = S_w = \frac{T_w}{T_{t_o}} - 1 \quad \text{at} \quad y = 0 \quad \text{for all} \quad x \tag{11}$$

$$S = S_i(y) \quad \text{at} \quad x = x_o \tag{12}$$

$$S = 0 \quad \text{at} \quad y = \infty \quad \text{for all} \quad x \tag{13}$$

The initial profiles, $u_i(y)$ and $S_i(y)$, will be specified in the Dorodnitsyn plane and will be taken as those given by the present solution for a flat plate with no pressure gradient. The velocity boundary condition at $y = \infty$, $u = u_1(x)$, will be calculated with the initial condition

$$u = u_1 = u_o \quad \text{at} \quad x = x_o \quad \text{and} \quad y = \infty \tag{14}$$

Referring to Figure 1(b), $u_1(x)$ will be calculated assuming free interaction from the beginning of the interaction, x_o, to the beginning of the plateau region and from the shock impingement point downstream. In the plateau region $u_1(x)$ will be held constant at the value at the beginning of the plateau.

Stewartson plane.- Equations (1), (2), and (7) are now transformed to an equivalent incompressible flow problem by means of the Stewartson transformation. The x,y-coordinates transform as follows

$$X = \int_o^x \frac{p_1 a_1}{p_o a_o}\, dx \qquad Y = \int_o^y \frac{\rho_1 a_1}{\rho_o a_o} \left(\frac{\rho}{\rho_1}\right) dy \tag{15}$$

and new velocity components are defined by

$$\left.\begin{aligned} u &= \frac{a_1}{a_o} U \\ v &= \frac{\rho_o}{\rho} \frac{p_1}{p_o} \frac{a_1}{a_o} V - \frac{\rho_o}{\rho} \frac{\partial Y}{\partial x} U \end{aligned}\right\} \tag{16}$$

It is assumed that the viscosity varies linearly with temperature

$$\frac{\mu}{\mu_o} = C \frac{T}{T_o} \tag{17}$$

and it is further assumed that C is unity. Equations (1), (2), and (7) become, respectively,

$$U \frac{\partial U}{\partial X} + V \frac{\partial U}{\partial Y} = (S + 1) U_1 \frac{\partial U_1}{\partial X} + \nu_o \frac{\partial^2 U}{\partial Y^2} \tag{18}$$

$$\frac{\partial U}{\partial X} + \frac{\partial V}{\partial Y} = 0 \tag{19}$$

$$U \frac{\partial S}{\partial X} + V \frac{\partial S}{\partial Y} = \nu_o \frac{\partial^2 S}{\partial Y^2} \tag{20}$$

The velocity boundary conditions, Equations (8) through (10), transform to

$$U = V = 0 \quad \text{at} \quad Y = 0 \quad \text{for all} \quad X \tag{21}$$

$$U = U_i(Y) \quad \text{at} \quad X = X_o \tag{22}$$

$$\left.\begin{aligned} U = U_1(X) &= \frac{a_o}{a_1} u_1(x) \\ \frac{\partial U}{\partial Y} &= 0 \end{aligned}\right\} \quad \text{at} \quad Y = \infty \quad \text{for all} \quad X \tag{23}$$

and the temperature boundary conditions, Equations (11) through (13), become

$$S = S_w = \frac{T_w}{T_{t_o}} - 1 \quad \text{at} \quad Y = 0 \quad \text{for all} \quad X \tag{24}$$

$$S = S_i(Y) \quad \text{at} \quad X = X_o \tag{25}$$

$$S = 0 \quad \text{at} \quad Y = \infty \quad \text{for all} \quad X \tag{26}$$

Dorodnitsyn plane.- The Dorodnitsyn transformation is now used to eliminate the viscosity and nondimensionalize the axial velocity component. The coordinate transformations are

$$\xi = \int_o^X \frac{U_1}{U_o} \frac{dX}{\ell} \qquad \eta = \frac{U_1}{U_o \ell} \sqrt{\frac{U_o \ell}{\nu_o}}\, Y \tag{27}$$

and the new velocity components are

$$\left.\begin{aligned} \bar{u} &= \frac{U}{U_1} \qquad \bar{v} = \frac{V}{U_1} \sqrt{\frac{U_o \ell}{\nu_o}} \\ \bar{w} &\equiv \bar{v} + \bar{u}\eta \frac{\dot{U}_1}{U_1} \end{aligned}\right\} \tag{28}$$

The "dot" indicates differentiation with respect to ξ. Under this transformation Equations (18) through (20) become

$$\bar{u}\frac{\partial \bar{u}}{\partial \xi} + \bar{w}\frac{\partial \bar{u}}{\partial \eta} = \left[(S+1) - \bar{u}^2\right]\frac{\dot{U}_1}{U_1} + \frac{\partial^2 \bar{u}}{\partial \eta^2} \tag{29}$$

$$\frac{\partial \bar{u}}{\partial \xi} + \frac{\partial \bar{w}}{\partial \eta} = 0 \tag{30}$$

$$\bar{u}\frac{\partial S}{\partial \xi} + \bar{w}\frac{\partial S}{\partial \eta} = \frac{\partial^2 S}{\partial \eta^2} \tag{31}$$

The velocity boundary conditions become

$$\bar{u} = \bar{v} = \bar{w} = 0 \quad \text{at} \quad \eta = 0 \quad \text{for all} \quad \xi \tag{32}$$

$$\bar{u} = \bar{u}_i(\eta) \quad \text{at} \quad \xi = \xi_o \tag{33}$$

$$\left.\begin{aligned} \bar{u} &= 1 \\ \frac{\partial \bar{u}}{\partial \eta} &= 0 \end{aligned}\right\} \quad \text{at} \quad \eta = \infty \quad \text{for all} \quad \xi \tag{34}$$

and the temperature boundary conditions become

$$S = S_w = \frac{T_w}{T_{t_o}} - 1 \quad \text{at} \quad \eta = 0 \quad \text{for all} \quad \xi \tag{35}$$

$$S = S_i(\eta) \quad \text{at} \quad \xi = \xi_o \tag{36}$$

$$S = 0 \quad \text{at} \quad \eta = \infty \quad \text{for all} \quad \xi \tag{37}$$

Integral Relations for Momentum and Energy

The reduction of Equations (29) through (31) to integral relations is done in exactly the same manner as described in Section 3.3 of Reference 2. With the assumption that $\partial\bar{u}/\partial\eta$ is only a function of $\bar{u}$, the first four moments of the momentum equation are

$$\left.\begin{aligned}
&\frac{d}{d\xi}\int_{\bar{u}_s}^{1}\frac{(1-\bar{u})\bar{u}\,d\bar{u}}{\frac{\partial\bar{u}}{\partial\eta}} = \bar{v}_s - \frac{\dot{U}_1}{U_1}\int_{\bar{u}_s}^{1}\frac{(S+1-\bar{u}^2)}{\frac{\partial\bar{u}}{\partial\eta}}\,d\bar{u} + \left.\frac{\partial\bar{u}}{\partial\eta}\right|_s \\
&-\frac{d}{d\xi}\int_{\bar{u}_s}^{1}\frac{(1-\bar{u})\bar{u}^2 d\bar{u}}{\frac{\partial\bar{u}}{\partial\eta}} = -\frac{\dot{U}_1}{U_1}\int_{\bar{u}_s}^{1}\frac{(S+1-\bar{u}^2)(1-2\bar{u})\,d\bar{u}}{\frac{\partial\bar{u}}{\partial\eta}} + \left.\frac{\partial\bar{u}}{\partial\eta}\right|_s - 2\int_{\bar{u}_s}^{1}\frac{\partial\bar{u}}{\partial\eta}\,d\bar{u} \\
&\frac{d}{d\xi}\int_{\bar{u}_s}^{1}\frac{(1-\bar{u})\bar{u}^3 d\bar{u}}{\frac{\partial\bar{u}}{\partial\eta}} = \frac{\dot{U}_1}{U_1}\int_{\bar{u}_s}^{1}\frac{(S+1-\bar{u}^2)(2-3\bar{u})\bar{u}\,d\bar{u}}{\frac{\partial\bar{u}}{\partial\eta}} - 2\int_{\bar{u}_s}^{1}(1-3\bar{u})\frac{\partial\bar{u}}{\partial\eta}\,d\bar{u} \\
&-\frac{d}{d\xi}\int_{\bar{u}_s}^{1}\frac{(1-\bar{u})\bar{u}^4 d\bar{u}}{\frac{\partial\bar{u}}{\partial\eta}} = -\frac{\dot{U}_1}{U_1}\int_{\bar{u}_s}^{1}\frac{(S+1-\bar{u}^2)(3-4\bar{u})\bar{u}^2 d\bar{u}}{\frac{\partial\bar{u}}{\partial\eta}} + 6\int_{\bar{u}_s}^{1}(1-2\bar{u})\bar{u}\frac{\partial\bar{u}}{\partial\eta}\,d\bar{u}
\end{aligned}\right\} \quad (38)$$

and the first moment of the energy equation is

$$\frac{d}{d\xi}\int_{\bar{u}_s}^{1}\frac{S(1-\bar{u})\bar{u}}{\frac{\partial\bar{u}}{\partial\eta}}\,d\bar{u} - (S\bar{v})_s = -\frac{\dot{U}_1}{U_1}\int_{\bar{u}_s}^{1}\frac{S(S+1-\bar{u}^2)}{\frac{\partial\bar{u}}{\partial\eta}}\,d\bar{u}$$

$$+\left(S\frac{\partial\bar{u}}{\partial\eta}\right)_s - \left(\frac{\partial S}{\partial\eta}\right)_s + 2\int_{\bar{u}_s}^{1}\frac{\partial S}{\partial\bar{u}}\frac{\partial\bar{u}}{\partial\eta}\,d\bar{u} \quad (39)$$

The limits of integration in the attached flow regions, that is, ahead of the separation point and downstream of the reattachment point, are the $\bar{u}$ velocities at the wall and at infinity, and in the separated region theu are the $\bar{u}$ velocities at the η_s line (the $\bar{u} = 0$ line) and at infinity. In both cases the limits are

0 to 1. The other terms must be evaluated either at the wall or the η_s line. The variable U_1 is made nondimensional by division with U_o.

Assumed Velocity and Temperature Profiles

Attached flow regions.- In the attached flow regions, that is, ahead of the separation point and downstream of the reattachment point, the assumed velocity profile is that which was used in References 1 and 2. The form used is

$$\frac{\partial \bar{u}}{\partial \eta} = \frac{(1 - \bar{u})\sqrt{\bar{u} + c_3}}{c_o + c_1 \bar{u} + c_2 \bar{u}^2} \tag{40}$$

The reasons for the choice of this particular form are given in Section 3.2 of Reference 1.

For the temperature profile, the form suggested in Section 3.4 of Reference 2 has been used. For second-order coupling the form is

$$S = S_w(1 - \bar{u}) + E_o(1 - \bar{u})\left(\sqrt{c_3} - \sqrt{\bar{u} + c_3}\right) \tag{41}$$

There are, therefore, four arbitrary parameters in the velocity profile, c_o, c_1, c_2, and c_3, and one in the temperature profile, E_o, which require five differential equations. These are obtained from the four moments of the momentum equation, Equation (38), and one moment of the energy equation, Equation (39). The final differential equations are obtained by substituting Equations (40) and (41) into Equations (38) and (39) and carrying out the required integrations and differentiations. The final equations are summarized in the appendices of this report.

Separated flow region.- In the separated flow region a distinction must be made between the inner and outer layers. The inner

layer is the reversed flow region between the wall and the $\bar{u} = 0$ line and the outer layer is the region from the $\bar{u} = 0$ line out to the edge of the boundary layer.

In the outer layer, Equation (40) is again used for the assumed velocity profile. The temperature profile is

$$S = S_s(1 - \bar{u}) + E_o(1 - \bar{u})\left(\sqrt{c_3} - \sqrt{\bar{u} - c_3}\right) \tag{42}$$

This differs from Equation (41) only in that the condition is imposed that $S = S_s$ at the $\bar{u} = 0$ line.

In the inner layer the velocity profile will be represented by a quadratic in η

$$\bar{u} = a + b\eta + c\eta^2 \tag{43}$$

To evaluate the constants the following conditions are imposed

$$\left.\begin{aligned} \bar{u} &= 0 \quad \text{at} \quad \eta = 0 \\ \bar{u} &= 0 \quad \text{at} \quad \eta = \eta_s \\ \frac{\partial \bar{u}}{\partial \eta} &= \alpha_s \quad \text{at} \quad \eta = \eta_s \end{aligned}\right\} \tag{44}$$

so that the inner layer velocity profile is given by

$$\bar{u} = -\alpha_s \eta \left(1 - \frac{\eta}{\eta_s}\right) \tag{45}$$

The total temperature profile is taken to be linear in the inner layer

$$S = a + b\eta \tag{46}$$

with the conditions

$$\left.\begin{aligned} S &= S_w \quad \text{at} \quad \eta = 0 \\ S &= S_s \quad \text{at} \quad \eta = \eta_s \end{aligned}\right\} \tag{47}$$

Equation (46) becomes

$$S = S_w + (S_s - S_w)\frac{\eta}{\eta_s} \tag{48}$$

It is noted that the next term in Equation (48) would be a cubic one. The quadratic term is zero since $\partial^2 S/\partial\eta^2$ is zero at the wall.

In the separated flow region there are eight arbitrary parameters in the assumed velocity and temperature profiles. They are

$$c_o,\ c_1,\ c_2,\ c_3,\ E_o,\ S_s,\ \alpha_s,\ \eta_s$$

Three equations are required in addition to the four moments of the momentum equation and the one moment of the energy equation. The three equations which will be used are obtained by matching first and second derivatives of the velocity profiles and the first derivative of the temperature profiles at the $\bar{u} = 0$ line. These equations are

$$\frac{\sqrt{c_3}}{c_o} = \alpha_s \tag{49}$$

$$\frac{c_3}{c_o^2}\left(-1 + \frac{1}{2c_3} - \frac{c_1}{c_o}\right) = \frac{2\alpha_s}{\eta_s} \tag{50}$$

$$-\frac{\sqrt{c_3}}{c_o}\left(S_s + \frac{E_o}{2\sqrt{c_3}}\right) = \frac{S_s - S_w}{\eta_s} \tag{51}$$

To obtain the differential equations these equations are differentiated with respect to ξ.

Pressure Boundary Conditions

The integral relations given by Equations (38) and (39) contain a term $\dot{U}_1$. This term is the derivative of the velocity at

the edge of the boundary layer with respect to ξ. To evaluate this term either a pressure distribution must be prescribed or the pressure distribution must be calculated simultaneously with the integration of the boundary layer equations. The present method calculates the pressure distribution assuming free interaction between the boundary layer and the inviscid flow. In applying the principle of free interaction, we assume that the pressure distribution on a body immersed in a viscous flow is the same as that on an equivalent body in an inviscid flow where the solid boundary of the original body has been augmented by the displacement thickness of the boundary layer.

The pressure is computed assuming free interaction from the beginning of interaction, x_o in Figure 1, to the point where the plateau pressure is reached, $dp/dx = 0$. From that point downstream to the shock-wave impingement point, the plateau pressure boundary condition is imposed, $dp/dx = \dot{U}_1 = 0$. Downstream of the impingement point free interaction is again assumed.

In the calculation of the pressure distribution under the assumption of free interaction, the Prandtl-Meyer relationship will be used. That is

$$\frac{dp_1}{p_1} = \frac{\gamma M_1^2}{\cos \phi_1 \sqrt{M_1^2 - \cos^2 \phi_1}} d\phi_1 \tag{52}$$

The angle $d\phi$ is the change in the angle of the external flow due to changes in the boundary-layer displacement thickness and to changes in slope of the surface. For a flat plate the quantities are related by

$$\frac{d\delta_o^*}{dx} + \frac{d\delta_i^*}{dx} = \tan \phi \tag{53}$$

where

δ_o^* = displacement thickness of the outer layer

δ_i^* = displacement thickness of the inner layer

In the unseparated regions δ_i^* is zero.

For the outer layer

$$\delta_o^* = \int_s^\infty \left(1 - \frac{\rho u}{\rho_1 u_1}\right) dy \tag{54}$$

where s is the y-coordinate of the $\bar{u} = 0$ line in the compressible plane (s = 0 in the unseparated regions). For the inner layer

$$\delta_i^* = \int_s^\infty \left(1 - \frac{\rho u}{\rho_1 u_1}\right) dy \tag{55}$$

The transformation of the above equations to the Dorodnitsyn plane yields the following integral relations

$$\frac{\delta_o^* \sqrt{R_o}}{(1 + m_o)} \left(\frac{1 + m_o}{1 + m_1}\right)^{(3\gamma-1)/2(\gamma-1)} = \frac{U_1 \ell}{U_o} \left[\int_o^1 \frac{S}{\frac{\partial \bar{u}}{\partial \eta}} d\bar{u} + \int_o^1 \frac{(1 - \bar{u})}{\frac{\partial \bar{u}}{\partial \eta}} d\bar{u} + \frac{m_1}{1 + m_1} \int_o^1 \frac{\bar{u}(1 - \bar{u})}{\frac{\partial \bar{u}}{\partial \eta}} d\bar{u} \right] \tag{56}$$

$$\frac{\delta_i^* \sqrt{R_o}}{(1 + m_o)} \left(\frac{1 + m_o}{1 + m_1}\right)^{(3\gamma-1)/2(\gamma-1)} = \frac{U_1 \ell}{U_o} \left[\int_o^{\eta_s} S \, d\eta + \int_o^{\eta_s} (1 - \bar{u}) d\eta + \frac{m_1}{1 + m_1} \int_o^{\eta_s} \bar{u}(1 - \bar{u}) d\eta \right] \tag{57}$$

where

$$m_1 = \frac{\gamma - 1}{2} M_1^2 \qquad M_1 = \frac{M_o \cos \phi_o}{\cos \phi_1} \frac{U_1}{U_o} \tag{58}$$

The expressions for the displacement thickness are found by substituting in the velocity and temperature profiles and carrying out the integrations.

Equation (53) requires the derivative of δ^* with respect to x. This is related to the derivative with respect to ξ, through the transformation, in the following way

$$\frac{d\delta^*}{dx} = \left(\frac{U_1}{U_o \ell}\right) \left(\frac{1 + m_o}{1 + m_1}\right)^{(3\gamma-1)/2(\gamma-1)} \frac{d\delta^*}{d\xi} \tag{59}$$

Method of Treating the Flow Across the Shock Impingement Point

A definite question arises as to the definition of the shock-wave impingement point; that is, the point in the boundary layer where the shock and the boundary layer interact. This point can range from one at the edge of the boundary layer to one at the wall. It is obvious that the point of intersection cannot lie beneath the sonic line since the flow from there to the wall is subsonic and consequently the pressure cannot rise discontinuously. The interaction model used in the present theory assumes for simplicity that the shock is reflected at the δ^* line. However, in the use of the theory for comparison with data the intersection of the shock wave with the "edge" of the boundary layer, obtained from schlieren pictures would probably be used for the impingement point or possibly the intersection of the shock wave extension with the wall. This indeterminancy in the experimental impingement point has an effect on comparisons between experiment and theory.

At the impingement point all of the variables in the Dorodnitsyn plane, c_o, c_1, c_2, c_3, E_o, and U_1, and η_s and S_s if the boundary

layer is separated, are assumed to be continuous. The effect of the shock wave striking the boundary layer is to turn the boundary layer toward the flat plate. This is accomplished by discontinuously changing the angle ϕ_1 in the free interaction equation, Equation (53). This change in ϕ_1 is the turning of the flow caused by the shock wave and the reflected expansion fan.

Let the angle ϕ just behind the shock be ϕ_4. From Equation (58) it is seen that unless $\phi_4 = -\phi_1$ a discontinuity in Mach number results. This discontinuity in Mach number results in discontinuities in all of the boundary-layer quantities (i.e., δ, δ^*, C_f, ..., etc.) in the physical, or compressible, plane. These discontinuities are small since $\phi_4 \simeq -\phi_1$ for laminar boundary layers. By an adjustment of some or all of the reference quantities at the impingement point, it is possible to make one or some of the quantities continuous across the shock. However, because of the way in which the Mach number and the reference quantities enter into the transformations, continuity of all the variables cannot be achieved in all planes. In the present investigation all quantities except ϕ_1 were made continuous in the Dorodnitsyn plane. An examination of the discontinuities in the physical plane show them to be quite small. For aesthetic reasons continuity of the quantities in the physical plane might be worth investigating.

Iteration Procedure to Determine Unique Solution

At the shock impingement point the angle ϕ_1 is changed discontinuously. With the beginning of interaction, x_o, and the impingement point, x_i, fixed it is not known what value of ϕ_4 right behind the shock will satisfy the downstream pressure boundary condition, $dp/dx = d^2p/dx^2 = 0$. This value of ϕ_4 must be determined by iteration. The iteration is built into the computer program and a typical set of results is shown in Figure 3. The pressure ratio p_1/p_o is plotted as a function of x for the region

downstream of the impingement point, $x_i = 0.075$ ft. For clarity the curves for iterations 3 through 8 are shown starting from their intersections with the curve for iteration 9. Upstream of the intersection points, these curves lie between the curves for iterations 1 and 2. The higher the iteration number the closer the curve is to iteration 9.

The results for the various iterations show two distinct behaviors. For iterations 1, 3, 5, 8, and 9, dp/dx is always positive and the solutions, if continued, would result in second separation points. This behavior is unallowable because no mechanism to induce a second separation point is present. For the other iterations the pressure reaches a maximum and then drops in a physically unrealistic fashion. The ends of these latter curves are shown dashed since the computations were actually stopped when dp/dx was equal to zero. As the value of ϕ_4 was determined more accurately the condition of $dp/dx = d^2p/dx^2 = 0$ was satisfied more closely. As can be seen from the curves the value of ϕ_4 which would satisfy this condition lies between the values used for iterations 7 and 9. For iteration 7 at an x of approximately 0.14 feet the condition of $dp/dx = 0$ was satisfied but d^2p/dx^2 was less than zero. For iteration 9 at $x \simeq 0.15$ ft., the condition of $d^2p/dx^2 = 0$ was satisfied but dp/dx was greater than zero.

For iteration 1 where ϕ_4 is much too small the boundary layer did not reattach. For iterations 3, 5, 8, and 9, where ϕ_4 is still too small, the boundary layer reattached but went to a second separation point. When ϕ_4 is too large, iterations 2, 4, 6, and 7, the boundary layer reattaches and the pressure reaches a maximum and then begins to decay. These characteristic behaviors were used for stopping the iterations. Once values of ϕ_4 which were too large and too small were known, the next guess was made by averaging the bracketing values. It can be seen that by increasing the accuracy on ϕ_4 the downstream pressure boundary condition becomes more closely satisfied. It appears not to be possible to converge exactly, with the present numerical integration scheme, because the determinant of the set of differential equations approaches zero at this point.

DIFFERENTIAL EQUATIONS

The differential equations solved by the computer program are presented in Appendix A for the attached flow regions and in Appendix B for the separated flow region. The steps in the derivation are not given, only the final equations. The derivations follow in the same manner as those in References 1 and 2.

Attached Flow Regions

The differential equations solved in the attached flow regions, ahead of separation and downstream of reattachment, are given in Appendix A. Equations (A-1) through (A-4) are the four moments of the momentum equation and are obtained by substituting the profiles of Equations (40) and (41) into the equations given in Equation (38) and performing the indicated integrations and differentiations. Equation (A-5) is the free-interaction equation and is obtained by using Equations (40), (41), (53), (56), (58), and (59) and the Prandtl-Meyer relationship

$$\dot{\phi}_1 = - \frac{\sqrt{M_1^2 - 1}}{2(1 + m_1)M_1^2} \frac{dM_1^2}{d\xi} \tag{60}$$

In the attached flow regions δ_i^* is zero. This resulting equation then has Equation (A-1) times $m_1/(1 + m_1)$ subtracted from it to give Equation (A-5). The one moment of the energy equation is given by Equation (A-6). This is obtained from Equation (39) using the profiles of Equations (40) and (41).

Separated Flow Region

The differential equations solved in the separated flow region are given in Appendix B. Equations (B-1) through (B-4) are the four moments of the momentum equation and are derived using

Equation (38) and the profiles specified by Equations((40) and (42). The next equation, Equation (B-5) is the free interaction equation. Equation (56) and the profiles of Equations (40) and (42) are used to evaluate δ_o^*. Equation (57) and the profiles of Equations (45) and (48) are used to determine δ_i^*. The derivatives of δ_o^* and δ_i^* are evaluated using Equations (58) through (60) and are substituted into Equation (53). Equation (B-5) is obtained by taking the resulting equation and subtracting $m_1/(1 + m_1)$ times Equation (B-1) from it. Equation (39) and the profiles of Equations (40) and (42) are used to determine the one moment of the energy equation, Equation (B-6). The last three differential equations, Equations (B-7) through (B-9) are obtained by rearranging Equations (49) through (51) and differentiating with respect to ξ.

In the computer program this set of nine equations has been reduced to a set of six. Equations (B-7) through (B-9) have been used to eliminate $\dot{\alpha}_s$, $\dot{\eta}_s$, and $\dot{S}_s$ from Equations (B-1) through (B-6). Equations (49) through (51) are used to evaluate α_s, η_s, and S_s.

Initial Values of the Variables

At the beginning of interaction, x_o, it is necessary that initial profiles be specified. The velocity profile, Equation (40), contains c_o, c_1, c_2, and c_3. In the present work the reference length, ℓ, will be taken equal to x_o so that

$$\frac{x_o}{\ell} = \frac{x_o}{\ell} = \xi_o = 1$$

It is assumed that the boundary layer ahead of the beginning of interaction behaves as a zero pressure gradient layer. Therefore, from Section 3.8 of Reference 2, the initial values of the c_n's will be taken as those for a Blasius profile at $\xi_o = 1$.

$$\left.\begin{aligned} c_o &= 3.157 \\ c_1 &= -1.923 \\ c_2 &= -0.3133 \\ c_3 &= 1.100 \end{aligned}\right\} \tag{61}$$

It is shown there that the Blasius profile in the incompressible plane is independent of wall temperature for no pressure gradient.

The temperature profile, Equation (41), contains the quantity E_o for which an initial value must be specified. For zero pressure gradient the Crocco relationship

$$S = S_w(1 - \bar{u}) \tag{62}$$

is valid. If E_o is set to zero in Equation (41), it reduces to the Crocco relationship. Since the assumption has been made that the boundary layer ahead of the beginning of interaction behaves as a zero pressure gradient layer, the initial condition on E_o is taken as

$$E_o = 0 \tag{63}$$

The initial condition for U_1/U_o is obtained by perturbing the pressure 0.1 percent from the value ahead of the beginning of interaction, $p_1/p_o = 1.001$. From the isentropic relationship

$$\frac{p}{p_t} = \left(1 + \frac{\gamma - 1}{2} M^2\right)^{-\gamma/(\gamma-1)} \tag{64}$$

and since $p_{t_1} = p_{t_o}$ the following expression for the initial value of U_1/U_o is obtained.

$$\left.\begin{aligned} \frac{U_1}{U_o} &= \frac{M_1 \cos \phi_1}{M_o \cos \phi_o} \simeq \frac{M_1}{M_o} \\ \left(\frac{M_1}{M_o}\right)^2 &= \frac{1}{\frac{\gamma - 1}{2} M_o^2} \left[\frac{1 + \frac{\gamma - 1}{2} M_o^2}{(1.001)^{(\gamma-1)/\gamma}} - 1 \right] \end{aligned}\right\} \quad (65)$$

An initial value of ϕ, ϕ_o, is required for the free-interaction equation. The expression used is that given in Section 3.8 of Reference 2.

$$\tan \phi_o = \frac{1}{\sqrt{R_o}} \left\{ 0.860823 \left[1 + S_w (1 + m_o) \right] + 1.193715\, m_o \right\} \quad (66)$$

During the computation ϕ_1 is determined from the integrated Prandtl-Meyer relationship

$$\phi_1 = -\sqrt{\frac{\gamma + 1}{\gamma - 1}} \tan^{-1} \sqrt{\frac{\gamma - 1}{\gamma + 1} \left(M_1^2 - 1 \right)} + \tan^{-1} \sqrt{M_1^2 - 1} + \phi_c \quad (67)$$

where

$$\phi_c = \phi_o + \sqrt{\frac{\gamma + 1}{\gamma - 1}} \tan^{-1} \sqrt{\frac{\gamma - 1}{\gamma + 1} \left(M_o^2 - 1 \right)} - \tan^{-1} \sqrt{M_o^2 - 1} \quad (68)$$

It is to be noted that the Mach number in the present work is defined parallel to δ^* whereas that used in References 1 and 2 was defined parallel to the x-axis.

The integration constant ϕ_c must be evaluated again at the shock impingement point since ϕ is changed discontinuously at this point. The expression is

$$\phi_c = \phi_4 + \sqrt{\frac{\gamma + 1}{\gamma - 1}} \tan^{-1} \sqrt{\frac{\gamma - 1}{\gamma + 1} \left(M_4^2 - 1 \right)} - \tan^{-1} \sqrt{M_4^2 - 1} \quad (69)$$

where

$$M_4 = \frac{M_o \cos \phi_o}{\cos \phi_4} \frac{U_1}{U_o} \tag{70}$$

EQUATIONS FOR QUANTITIES OUTPUT BY COMPUTER PROGRAM

The equations for the quantities output by the computer program will now be given without derivation. The definitions in the compressible plane will be given followed by the equations obtained by going through the transformations to the Dorodnitsyn plane.

Axial Distance

The axial distance, x, in feet, is obtained by integration of the following differential equation

$$x = x_o + \ell \int_{\xi_o}^{\xi} \frac{\left(\frac{1 + m_1}{1 + m_o}\right)^{(3\gamma-1)/2(\gamma-1)}}{\frac{U_1}{U_o}} d\xi \qquad (71)$$

Distance from the Flat Plate to the $\overline{u} = 0$ Line

In the attached flow regions the distance from the flat plate to the $\overline{u} = 0$ line, s, in feet, is

$$s = 0 \qquad (72)$$

In the separated region

$$s = y\Big|_{\overline{u}=o} \qquad (73)$$

so that

$$s = \frac{\ell}{\frac{U_1}{U_o}\sqrt{R_o}} \left(\frac{1 + m_1}{1 + m_o}\right)^{(\gamma+1)/2(\gamma-1)} \left[(1 + m_1)\eta_s \left(1 + \frac{S_s + S_w}{2}\right) - \frac{m_1 \alpha_s^2 \eta_s^3}{30}\right] \qquad (74)$$

Boundary-Layer Displacement Thickness

The boundary-layer displacement thickness, δ^*, in feet, is given by

$$\delta^* = \int_0^\infty \left(1 - \frac{\rho u}{\rho_1 u_1}\right) dy \tag{75}$$

In the attached flow regions

$$\delta^* = \frac{\ell}{\frac{U_1}{U_o}\sqrt{R_o}} \left(\frac{1 + m_1}{1 + m_o}\right)^{(\gamma+1)/2(\gamma-1)} \left[(1 + m_1)\left(\overline{H}_1 - E_o\overline{N}_o + \overline{f}_1\right) + m_1\overline{f}_2\right] \tag{76}$$

and in the separated region

$$\delta^* = \frac{\ell}{\frac{U_1}{U_o}\sqrt{R_o}} \left(\frac{1 + m_1}{1 + m_o}\right)^{(\gamma+1)/2(\gamma-1)} \left\{(1 + m_1)\left[\left(\tilde{H}_1 - E_o\overline{N}_o + \overline{f}_1\right) + \eta_s\left(1 + \frac{S_s + S_w}{2}\right) + \frac{\eta_s^2\alpha_s}{6}\right] + m_1\left[\overline{f}_2 - \frac{\eta_s^2\alpha_s}{6}\left(1 + \frac{\eta_s\alpha_s}{5}\right)\right]\right\} \tag{77}$$

Boundary-Layer Momentum Thickness

The boundary-layer momentum thickness, δ^{**}, in feet, is given by

$$\delta^{**} = \int_0^\infty \frac{\rho u}{\rho_1 u_1}\left(1 - \frac{u}{u_1}\right) dy \tag{78}$$

In the attached flow regions

$$\delta^{**} = \frac{\ell}{\frac{U_1}{U_o}\sqrt{R_o}} \left(\frac{1 + m_1}{1 + m_o}\right)^{(\gamma+1)/2(\gamma-1)} \overline{f}_2 \tag{79}$$

and in the separated flow region

$$\delta^{**} = \frac{\ell}{\frac{U_1}{U_o}\sqrt{R_o}} \left(\frac{1 + m_1}{1 + m_o}\right)^{(\gamma+1)/2(\gamma-1)} \left[\overline{f}_2 - \frac{\eta_s{}^2 \alpha_s}{6}\left(1 + \frac{\eta_s \alpha_s}{5}\right)\right] \tag{80}$$

Local Reynolds Number

The local Reynolds number is defined as

$$R_x = \frac{\rho_1 u_1 x}{\mu_1} \tag{81}$$

so that in all regions it is

$$R_x = R_o \frac{x}{\ell} \frac{U_1}{U_o} \left(\frac{1 + m_1}{1 + m_o}\right)^{(\gamma-3)/2(\gamma-1)} \tag{82}$$

Mach Number at the Edge of the Boundary Layer

In all regions the Mach number is

$$M_1 = \frac{M_o \cos \phi_o}{\cos \phi_1} \frac{U_1}{U_o} \tag{83}$$

Pressure, Density, and Velocity Ratios

In all regions the pressure ratio is,

$$\frac{p_1}{p_o} = \left(\frac{1 + m_o}{1 + m_1}\right)^{\gamma/(\gamma-1)} \tag{84}$$

the density ratio is,

$$\frac{\rho_1}{\rho_o} = \left(\frac{1 + m_o}{1 + m_1}\right)^{1/(\gamma-1)} \tag{85}$$

and the axial velocity ratio is

$$\frac{u_1}{u_o} = \sqrt{\frac{1 + m_o}{1 + m_1}}\ \frac{U_1}{U_o} \tag{86}$$

Stanton Number

The Stanton number, St, is determined from the following two definitions of heat-transfer rate, q,

$$\left.\begin{aligned} q &= k_w \left.\frac{\partial T}{\partial y}\right|_w \\ \text{and} \qquad q &= \rho_1 u_1 St\ c_p \left(T_{t_o} - T_w\right) \end{aligned}\right\} \tag{87}$$

so that

$$St = \frac{k_w \left.\frac{\partial T}{\partial y}\right|_w}{\rho_1 u_1 c_p \left(T_{t_o} - T_w\right)} \tag{88}$$

In the attached flow regions

$$St = \frac{1}{\sqrt{R_o}} \left(\frac{1 + m_o}{1 + m_1} \right) \left(\frac{\sqrt{c_3}}{c_o} + \frac{E_o}{2c_o S_w} \right) \tag{89}$$

and in the separated region

$$St = - \frac{1}{\sqrt{R_o}} \left(\frac{1 + m_o}{1 + m_1} \right) \left(\frac{S_s - S_w}{\eta_s S_w} \right) \tag{90}$$

For an adiabatic wall this quantity is not calculated.

Heat-Transfer Rate Ratio

From Equation (87) the heat-transfer rate ratio, q_1/q_o, is

$$\frac{q_1}{q_o} = \frac{\rho_1 u_1}{\rho_o u_o} \frac{St}{St_o}$$

or

$$\frac{q_1}{q_o} = \left(\frac{1 + m_o}{1 + m_1} \right)^{(\gamma+1)/2(\gamma-1)} \frac{U_1}{U_o} \frac{St}{St_o} \tag{91}$$

For an adiabatic wall this is not computed.

Skin-Friction Coefficient

The skin-friction coefficient, C_f, is defined by

$$C_f = \frac{\tau_w}{\frac{1}{2} \rho_1 u_1^2} \tag{92}$$

In the attached flow regions, this becomes

$$C_f = \frac{2}{\sqrt{R_o}} \left(\frac{1 + m_o}{1 + m_1} \right) \frac{\sqrt{c_3}}{c_o} \tag{93}$$

and in the separated region

$$c_f = -\frac{2}{\sqrt{R_o}}\left(\frac{1 + m_o}{1 + m_1}\right)\alpha_s \tag{94}$$

Boundary-Layer Profiles

The computer program also outputs a number of profiles through the boundary layer as a function of $\bar{u}$ where

$$\bar{u} = \frac{u}{u_1} \tag{95}$$

In presenting the equations used to calculate the profiles, those used in the inner layer, from the wall to the $\bar{u} = 0$ line, and those used in the outer layer, from the $\bar{u} = 0$ line to the edge of the boundary layer, are given separately.

Variation of $\bar{u}$.- The $\bar{u}$ variation in the inner layer is obtained by picking a value of η and using Equation (45) to calculate the corresponding value of $\bar{u}$. In the outer layer the value of $\bar{u}$ is picked.

Variation of y.- The variation of y, the distance through the boundary layer from the wall in feet, in the inner layer is given by

$$y = \frac{\ell}{\frac{U_1}{U_o}\sqrt{R_o}}\left(\frac{1+m_1}{1+m_o}\right)^{(\gamma+1)/2(\gamma-1)}\left[(1+m_1)(S_w+1)\eta + \frac{(1+m_1)(S_s - S_w)}{2\eta_s}\eta^2 - m_1\eta^3\alpha_s{}^2\left(\frac{1}{3} - \frac{\eta}{2\eta_s} + \frac{\eta^2}{5\eta_s{}^2}\right)\right] \tag{96}$$

where η was assumed in order to calculate $\bar{u}$.

In the outer layer the following expression is used.

$$y = y\Big|_{\eta=\eta_s} + \frac{\ell}{\frac{U_1}{U_o}\sqrt{R_o}} \left(\frac{1 + m_1}{1 + m_o}\right)^{(\gamma+1)/2(\gamma-1)} \Bigg\{ (\eta - \eta_s) + m_1 \left[c_o F_o + (c_o + c_1) F_1 + (c_1 + c_2) F_2 + c_2 F_3\right] + (1 + m_1) \left[\left(S_s + E_o\sqrt{c_3}\right)(c_o F_o + c_1 F_1 + c_2 F_2) - E_o\left(c_o \bar{u} + c_1 \frac{\bar{u}^2}{2} + c \frac{\bar{u}^3}{3}\right)\right]\Bigg\} \tag{97}$$

where

$$(\eta - \eta_s) = \frac{(c_o + c_1 + c_2)}{\sqrt{1 + c_3}} \log\left[\frac{\left(\sqrt{\bar{u} + c_3} + \sqrt{1 + c_3}\right)\left(\sqrt{c_3} - \sqrt{1 + c_3}\right)}{\left(\sqrt{\bar{u} + c_3} - \sqrt{1 + c_3}\right)\left(\sqrt{c_3} + \sqrt{1 + c_3}\right)}\right] - (c_1 + c_2) F_o - c_2 F_1 \tag{98}$$

and

$$F_o = 2\left(\sqrt{\bar{u} + c_3} - \sqrt{c_3}\right)$$

$$F_n = \frac{2}{1 + 2n}\left(\bar{u}^n\sqrt{\bar{u} + c_3} - n c_3 F_{n-1}\right) \qquad n = 1,2,3 \tag{99}$$

In the attached flow regions $y\Big|_{\eta=\eta_s}$ is zero in Equation (97) and S_s is replaced by S_w in the same equation.

Dimensionless velocity derivative.- The dimensionless velocity derivative is evaluated using the following equation

$$\frac{d\bar{u}}{d\left(\frac{y}{\ell}\right)} = \frac{U_1}{U_o}\sqrt{R_o}\left(\frac{1 + m_o}{1 + m_1}\right)^{(\gamma+1)/2(\gamma-1)} \left[\frac{1}{(S + 1)(1 + m_1) - m_1\bar{u}^2}\right] \frac{\partial\bar{u}}{\partial\eta} \tag{100}$$

In the attached flow regions, Equations (40) and (41) are used to evaluate $\partial\bar{u}/\partial\eta$ and S. For the inner layer in the separated region, Equation (48) is used to evaluate S and the first derivative of Equation (45)

$$\frac{\partial\bar{u}}{\partial\eta} = -\alpha_s + \frac{2\alpha_s}{\eta_s}\eta \tag{101}$$

is used for $\partial\bar{u}/\partial\eta$. For the outer layer in the separated region Equations (40) and (42) are used.

Temperature profiles.- Two temperature profiles are calculated. They are the ratio of the local stagnation temperature to the stagnation temperature at the edge of the boundary layer and the ratio of the local static temperature to the local stagnation temperature. The first of these T_t/T_{t_o} is computed using the appropriate assumed temperature profile, either Equation (40), (42), or (48), for S. Then

$$\frac{T_t}{T_{t_o}} = S + 1 \tag{102}$$

The second ratio, T/T_t, is given by

$$\frac{T}{T_t} = \frac{1}{(S+1)}\left[(S+1) - \frac{m_o}{1+m_1}\left(\frac{U_1}{U_o}\right)^2 \bar{u}^2\right] \tag{103}$$

Mach number.- The Mach number is calculated from the temperature ratio of Equation (103). The isentropic relationship is

$$\frac{T_t}{T} = \left(1 + \frac{\gamma - 1}{2} M^2\right)$$

or

$$M = \pm\sqrt{\frac{2}{\gamma - 1}\left(\frac{T_t}{T} - 1\right)} \tag{104}$$

The plus sign is used in the outer layer and the minus sign is used in the inner layer to represent reversed flow.

Mass flow.- A dimensionless boundary layer mass flow, $\overline{\Psi}$, is also calculated. This quantity is defined as

$$\overline{\Psi} = \frac{\Psi}{\mu_o\sqrt{R_o}} = \frac{1}{\mu_o\sqrt{R_o}} \int_o^y \rho u \, dy \tag{105}$$

In the inner layer

$$\overline{\Psi} = -\frac{\alpha_s \eta^2}{2} + \frac{\alpha_s \eta^3}{3\eta_s} \tag{106}$$

and in the outer layer

$$\overline{\Psi} = \overline{\Psi}_{\eta=\eta_s} - (c_o + c_1 + c_2)\left\{F_o - \frac{1}{\sqrt{1+c_3}} \log\left[\frac{\left(\sqrt{\bar{u}+c_3}+\sqrt{1+c_3}\right)\left(\sqrt{c_3}-\sqrt{1+c_3}\right)}{\left(\sqrt{\bar{u}+c_3}-\sqrt{1+c_3}\right)\left(\sqrt{c_3}+\sqrt{1+c_3}\right)}\right]\right\}$$
$$- (c_1 + c_2)F_1 + c_2 F_2 \tag{107}$$

The F_n's are obtained from Equation (99). In the attached flow region, $\overline{\Psi}_{\eta=\eta_s}$ is zero. It is evaluated using Equation (106) in the separated region.

INPUT DATA REQUIRED BY COMPUTER PROGRAM

The input data deck required by the computer program consists of three cards. These cards are shown in Figure 4. In this figure the variable is given as well as the card column in which the value of the variable is begun and the format in which it is punched. All of the variables have positive values with the exception of the last two in the last card which are either negative or zero. The card column shown for these is the column in which the minus sign is to be punched. For all of the others it is the column in which the first digit is punched.

The first quantity in Card No. 1 is the Reynolds number per foot, R_o/ℓ, based on conditions at the edge of the boundary layer at the beginning of interaction. Since the reference length, ℓ, is taken equal to x_o,

$$\frac{R_o}{\ell} = \frac{R_o}{x_o} = \frac{\rho_o u_o}{\mu_o} \quad \text{per foot}$$

The next quantity is the Mach number, M_o, at the edge of the boundary layer at the beginning of interaction. These two quantities should be known as accurately as possible. The third quantity on the first card is the ratio of specific heats, γ. The last parameter is T_w/T_{t_o}. This is the ratio of the temperature of the flat plate to the stagnation temperature at the edge of the boundary layer at the beginning of interaction.

The next card contains four quantities. The first of these is the location of the beginning of interaction, x_o, measured in feet from the leading edge of the flat plate. This is the point where the pressure is assumed to have risen 0.1 percent from the flat-plate value. The next parameter is the shock-wave impingement point, x_i, measured in feet from the leading edge of the flat plate. This could be the point where the shock strikes the edge of the boundary layer, the flat plate, or any point in

between. No attempt has been made in the present work to define the point in the boundary layer which should be used. The program will not use this point exactly as input. It uses as the impingement point the value of x at the end of the first integration step where $x \geq x_i$. Thus, the actual x_i may be larger than the one which was input. The third quantity in Card No. 3 is the output interval, Δx_{print}, in feet. Output will only be printed this frequently and not at the end of each integration step. The last quantity is an index controlling the amount of output. The solution downstream of the shock-wave impingement point requires an iteration on ϕ_4 until the downstream pressure boundary condition is satisfied. Normally the output from the last iteration would be all that would be of interest, however, in certain instances the results of each iteration may be wanted. The quantity NOUT controls this. If NOUT = 0 then only the results of the last iteration will be printed. If NOUT = 1 the results of all iterations will be printed.

The first quantity on the third card, PHITOL, specifies how accurate ϕ_4 is to be determined and, therefore, how close the downstream pressure boundary condition, $dp/dx = d^2p/dx^2 = 0$, is satisfied. The range on PHITOL is normally from 10^{-3} to 10^{-5}. For preliminary runs 10^{-3} is sufficient to determine the final pressure level downstream of the impingement point. Since ϕ_4 and M_4 are known and if it is assumed that the final ϕ is zero, the final pressure can be found from the Prandtl-Meyer angle and tables such as Reference 6. Once the desired final pressure has been obtained the computation can be restarted with PHITOL equal to 10^{-5} and the more accurate solution obtained. For the example shown in Figure 3, the iteration would have been terminated at iteration 8 for PHITOL = 10^{-3}. The solution is terminated at the end of the iteration where PHITOL is satisfied.

The last two quantities, PHHI and PHLO, on Card No. 3 are the bracketing values of ϕ_4 determined by the iteration. They must be input as zero unless the computation is being restarted using

the results of a previous run. As an example again consider Figure 3. When the computation was first started, PHHI and PHLO were input as zero. Let us assume PHITOL was input as 10^{-3} so that the last iteration would have been iteration 8. In order to determine the solution more accurately, we wish to restart the computation with iteration 8 with PHITOL equal to 10^{-5}. From the computer output for iteration 8 we obtain PHHI and PHLO. PHHI is given as -0.138345 and PHLO as -0.137095. These values are then input, iteration 8 is repeated, and additional iterations computed until PHITOL is satisfied. This restart procedure can also be used if the computation is stopped for any other reason, for example, the time estimate is exceeded.

The quantities PHHI and PHLO are given on the first page of output for each iteration which is indicated by "Impingement point - Values behind shock" printed at the top of the page. If only output from the last iteration is requested, NOUT = 0, and the computation is stopped because of exceeding the time estimate or some other similar reason, the two numbers can be obtained from the last page of output where they are tabulated for each iteration. The last pair of values should be used.

USE OF COMPUTER PROGRAM AND COMPARISONS WITH DATA

In order to assess the accuracy of the theory and also to demonstrate the use of the computer program, comparisons have been made between experiment and theory for a limited number of sets of experimental data. The results of these comparisons are presented in Figures 5 through 8. In the discussion which follows it is assumed that the conditions at the edge of the boundary layer at the beginning of the interaction, R_o/x_o, M_o, and T_{t_o}, are known as well as the location of the shock-wave impingement point, x_i, and the temperature of the plate, T_w. These quantities may be determined by a simple inviscid calculation or by iterating between a method of characteristics solution and an attached boundary-layer solution. The latter method is desirable at hypersonic speeds since the boundary-layer displacement thickness can have a significant effect on R_o and M_o. It should definitely be used when the inviscid flow field is known to be nonuniform or contains intersecting shock waves (i.e., hypersonic inlets) since x_i can be significantly changed by these factors.

Two quantities still remain to be determined, the location of the beginning of interaction and the shock-wave strength. These two quantities are not independent and their treatment in an actual computation depends on whether it is desired to fit experimental data or to predict a separated flow. The change in the inclination, ϕ, of the δ^* line at shock impingement depends on the shock-wave strength. As the program is now written, a value of x_o is specified as input and an iterative calculation is made downstream of shock impingement to determine the value of ϕ_4 for which the downstream pressure boundary condition $dp/dx = d^2p/dx^2 = 0$ is satisfied. This yields a value of the downstream plateau pressure. If this value of the plateau pressure is not compatible with the value for a known shock strength, then x_o is varied until the final plateau pressure has the proper value. If the plateau pressure

is too low, the value of x_o is reduced, and conversely. This procedure is the prediction method. If the value of x_o and x_i are known from experiment, then these quantities are used as input to perform a data-fitting calculation and to calculate the downstream plateau pressure. This would be done if the shock strength is unknown. Comparison is then made between the theoretical and experimental pressure distributions. In particular, comparison would be made between the final plateau pressures. This procedure is the data-fitting method. Examples of the use of the program for both purposes are given in the following paragraphs.

Figure 5 shows the results of using the program as a prediction technique. The values of M_o and R_o/x_o are taken from Figure 18(a) of Reference 7 as well as the inviscid flow final pressure level and the impingement point, x_i. A first guess of $x_o = 0.0155$ ft. was made which resulted in a low final pressure. The next guess was $x_o = 0.0075$ ft. The final pressure was too high. A third guess of $x_o = 0.115$ ft. resulted in a final pressure which matched the inviscid one. The experimental data are also shown in Figure 5. The calculated pressure distribution through the separation point agrees quite well with the data. The calculated plateau pressure ahead of the impingement point is below that obtained experimentally, $p_1/p_o = 1.37$ as compared to the experimental value of about 1.43. Downstream of the impingement point the pressure gradient is somewhat steeper than that shown by the data when the final pressure level is matched. The iteration on x_o is not built into the program.

Figure 6 shows the results obtained when the theory was used for data fitting and compared with the data of Figure 8(c) of Reference 8. The shock generator angle was not known. This case was selected since the skin-friction data and the velocity profiles indicated that the flow was laminar up to the point where the final pressure was reached. Figure 6(a) presents the pressure data comparisons. Two theoretical curves are shown. In one, $x_o = 0.115$ ft., the pressure data through separation was matched. This results in

a low final pressure. In the other, x_o = 0.105 ft., the final pressure was matched. When this is done, the calculated separation point is upstream of that found experimentally. Figure 6(b) shows the skin-friction comparisons for the same two cases. Ahead of the impingement point, x_i, the agreement is better when the pressure data through separation are matched, x_o = 0.115 ft. Downstream of x_i this also appears to be true. However, the data show reattachment taking place between x = 0.208 ft. and 0.216 ft. With x_o = 0.115 ft., reattachment occurs at 0.192 feet. When the final pressure is matched, x_o = 0.105 ft., reattachment occurs at 0.208 feet which agrees with the data. Figure 6(c) compares the calculated velocity profiles with those measured experimentally. For both values of x_o, the calculated profiles agree well with the data except for x = 0.184 ft. This is in the separated region. When the separation region pressure is not matched the reversed flow region is too large. This must clearly be the case near the separation point if the separation point is not predicted exactly.

In Figure 7 comparisons are made with the data of Figure 8(e) of Reference 8. This case is one which is transitional downstream of the shock impingement point as clearly shown by the experimental skin friction and velocity profiles. Even though the theory is not valid for this case downstream of transition, the computations were made to see how the theory agreed with experiment upstream of transition. Only one curve is shown, namely, that for which the data through the separation point have been matched. For curiousity sake, an attempt was made to match downstream pressure. This was not possible without starting the interaction close to the leading edge. A computation made with x_o = 0.005 ft. yielded a final pressure ratio between 1.8 and 1.9.

It is seen in Figure 7 that the calculated pressure ratio, skin friction, and velocity profiles all agree well with the data up to the impingement point. Downstream of this point the agreement is very poor. It thus appears that even though transition

occurs downstream of the shock impingement point the boundary layer up to this point exhibits laminar characteristics.

Figure 8 presents comparisons with two sets of unpublished data obtained from NASA Ames Research Center. These data were obtained on the configuration shown in the following sketch:

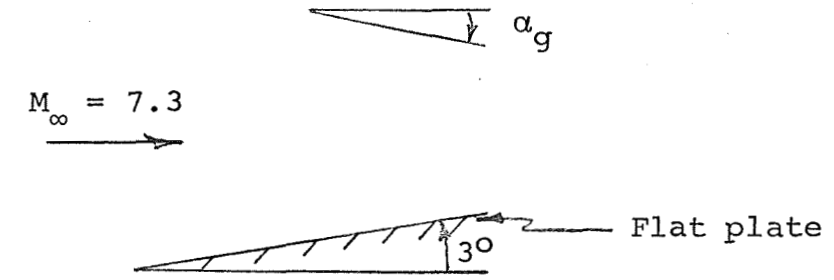

The wall of the flat plate is highly cooled. The quantities R_o/x_o and M_o have been obtained from a characteristics solutions.[1] For the weak shock-wave case, Figure 8(a), the agreement between the theoretical curve and the data is good over the entire interaction region. The strong shock case exhibits the same behavior as the case shown in Figure 7(a). The pressures agree fairly well up to the impingement point. Downstream of this point the theoretical pressure is far below the experimental pressure indicating that this flow may also be transitional.

It is noted that the calculated final pressure rise in Figure 6(a) for the case where the data through separation were matched was considerably below that obtained experimentally. Where the flow was known to be laminar (Figs. 5 and 8(a)), this pressure was matched when the data through separation were matched. This was not the case for the set of data known to be transitional (Fig. 7(a)). Consequently, the lack of agreement in Figure 6(a) may be due either to inaccuracy of the theory or transition of the boundary layer.

---

[1]The large difference between M_∞ and M_o is an indication of the nonuniformity of the inlet flow.

CONCLUDING REMARKS

(1) The present report presents a method for calculating laminar boundary layer-shock wave interactions by the method of integral relations. Second-order temperature coupling between the temperature and velocity profiles is used so that the method is applicable to highly-cooled walls of any uniform temperature. No comparable method has been published to the knowledge of the authors.

(2) A criterion has been developed to determine the unique solution, for a given Reynolds number, Mach number, wall temperature, and shock-wave impingement point based on certain prescribed downstream pressure boundary conditions. These conditions are that when a specified final pressure is attained downstream of the impingement point, both the first and second derivatives of pressure with respect to distance shall be zero.

(3) A computer program has been written based on the theory for a flat-plate configuration. An iterative solution is carried out downstream of the shock impingement point to determine the solution which satisfies the downstream pressure first and second derivative boundary conditions for a prescribed position of the beginning of interaction.

(4) The program can be used as a prediction technique as well as a data-matching technique. If the shock-wave impingement point and strength are known, the beginning of interaction can be iterated on, by making a series of runs with the computer program, until not only the downstream pressure first and second derivative boundary conditions are satisfied but also the final pressure level consistent with the shock strength is matched.

(5) A limited number of comparisons between experiment and theory have been made for pressure distributions, velocity profiles, and skin-friction distributions. For data which are known to be laminar throughout the entire interaction region, the agreement is reasonably good. For data known to be transitional downstream of

the shock-wave impingement point, the theory matches the data upstream of this point reasonably well.

(6) Insufficient comparisons have been made between the theory and data known to be laminar throughout the entire interaction region to fully assess the accuracy of the theory.

(7) The program will yield heat-transfer rates in the interaction region, but no comparison between experiment and theory has been made to assess the accuracy of the heat-transfer predictions.

RECOMMENDATIONS FOR FUTURE WORK

(1) A comparison of the theory with all data known to be laminar over the entire interaction region should be made in order to evaluate the accuracy of the theory further.

(2) The present method allows small discontinuities in boundary-layer thickness, displacement thickness and momentum thickness, and other quantities across the shock impingement point. For simplicity these quantities have been made continuous in the Dorodnitsyn plane with the result that they are not continuous in the compressible plane. While these discontinuities are small, further work may be possible to improve the elegance of the present method by making some or possibly all of the physical quantities continuous in the compressible plane.

(3) The computer program should be modified to handle two-dimensional configurations other than flat plates. This modification requires coupling a prescribed pressure distribution program to the existing program if the configuration is not a flat plate prior to the beginning of interaction.

(4) For external flow fields which are nonuniform, such as those that exist in inlets, it is necessary to couple an inviscid flow field program to the boundary-layer program so that conditions at the edge of the boundary layer at the beginning of interaction and the shock strength at impingement can be determined.

(5) The limited amount of data examined in the present investigation indicates that boundary-layer transition at shock impingement may be significant for the shock strengths typical of hypersonic inlet design. Since a method for treating this transitional case appears technologically important, an analysis for this case is recommended. The fact that the laminar analysis appears valid up to shock impingement for the transitional cases examined suggests an approach to the transitional case.

(6) There appears to be a tendency in the present method to predict the first plateau pressure somewhat low. It is possible

to improve the accuracy of this prediction by use of cubic profiles to describe the reversed flow, but increased computer running time will result.

REFERENCES

1. Nielsen, J. N., Lynes, L.L., and Goodwin, F. K.: Calculation of Laminar Separation with Free Interaction by the Method of Integral Relations, Part I - Two-Dimensional Supersonic Adiabatic Flow. AFFDL-TR-65-107, Oct. 1965.

2. Nielsen, J. N., Lynes, L. L., and Goodwin, F. K.: Calculation of Laminar Separation with Free Interaction by the Method of Integral Relations, Part II - Two-Dimensional Supersonic Non-adiabatic Flow and Axisymmetric Supersonic Adiabatic and Non-adiabatic Flows. AFFDL-TR-65-107, Part II, Jan. 1966.

3. Reyhner, T. A. and Flügge-Lotz, I.: The Interaction of a Shock Wave with a Laminar Boundary Layer. Tech. Rep. No. 163, Division of Engineering Mechanics, Stanford Univ., Stanford, Calif., Nov. 1966.

4. Dorodnitsyn, A. A.: General Method of Integral Relations and Its Application to Boundary-Layer Theory. Advance in Aero. Sci., vol. 3, Von Kármán Ed., 1962.

5. Howarth, L.: Modern Developments in Fluid Dynamics. High Speed Flow, vol. 1, Oxford, 1956.

6. Ames Research Staff: Equations, Tables, and Charts for Compressible Flow. NACA Rep. 1135, 1953.

7. Chapman, D. R., Kuehn, D. M., and Larson, H. K.: Investigation of Separated Flows in Supersonic and Subsonic Streams with Emphasis on the Effects of Transition. NACA TN 3869, Mar. 1957.

8. Hakkinen, R. J., Greber, I., Trilling, L., and Abarbanel, S. S.: The Interaction of an Oblique Shock Wave with a Laminar Boundary Layer. NASA Memo 2-18-59W, Mar. 1959.

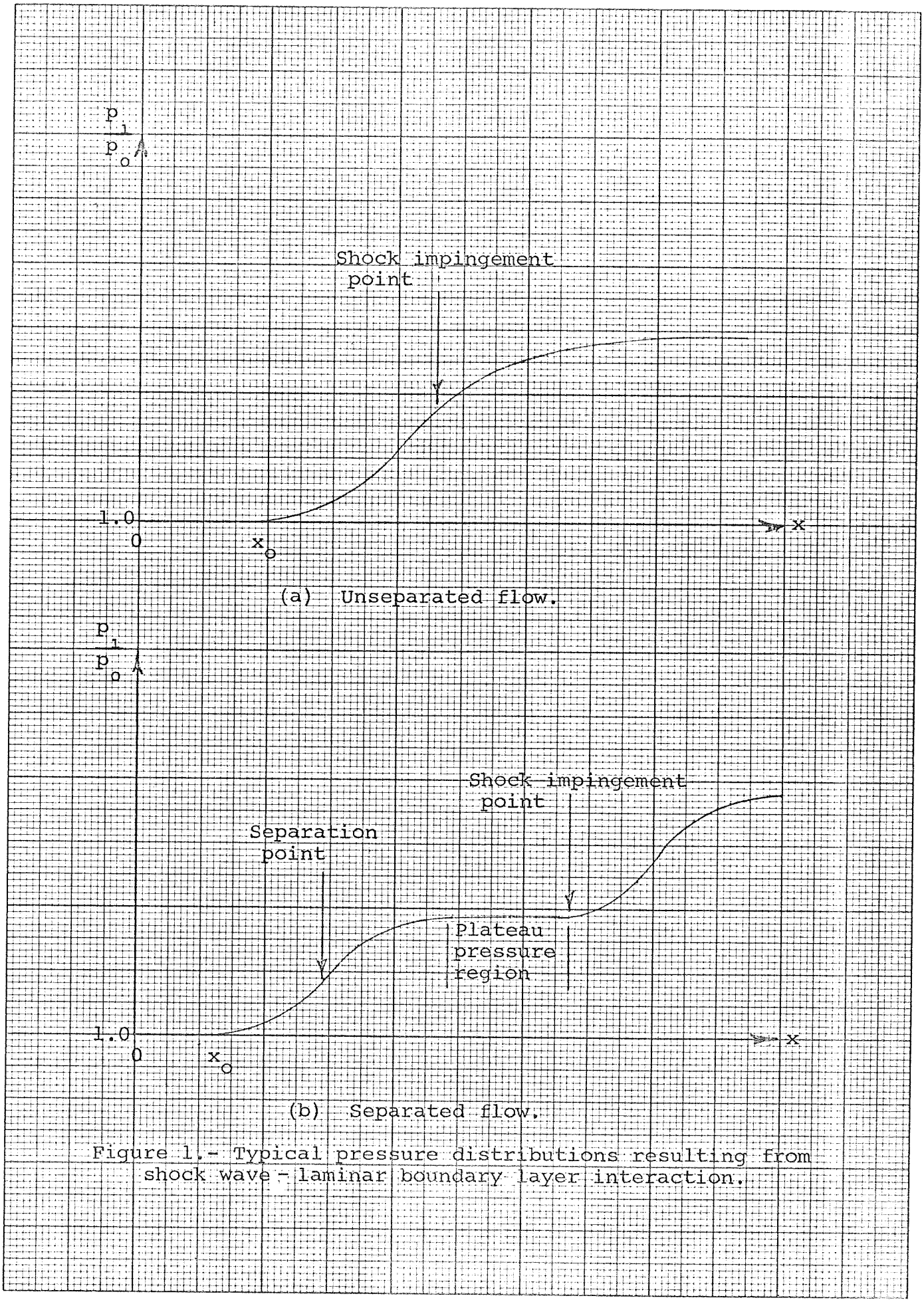

Figure 1.- Typical pressure distributions resulting from shock wave - laminar boundary layer interaction.

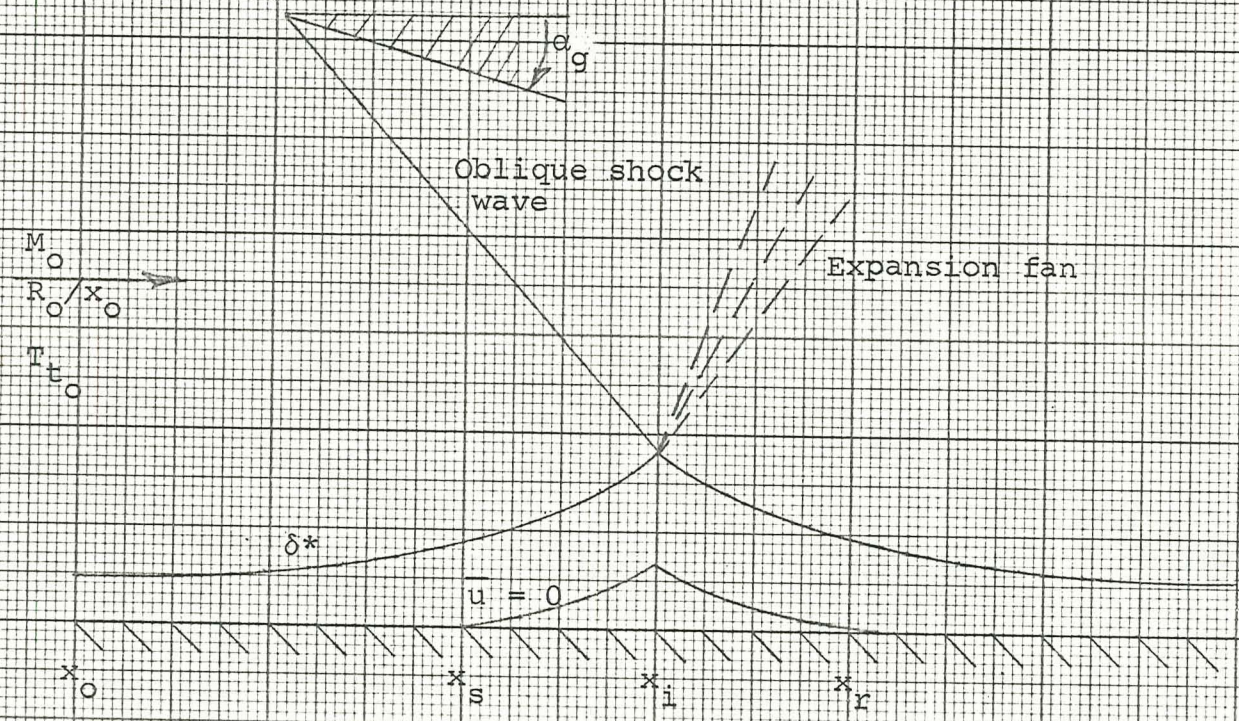

Figure 2.- Separated laminar flow on a flat plate as a result of shock wave--boundary-layer interaction.

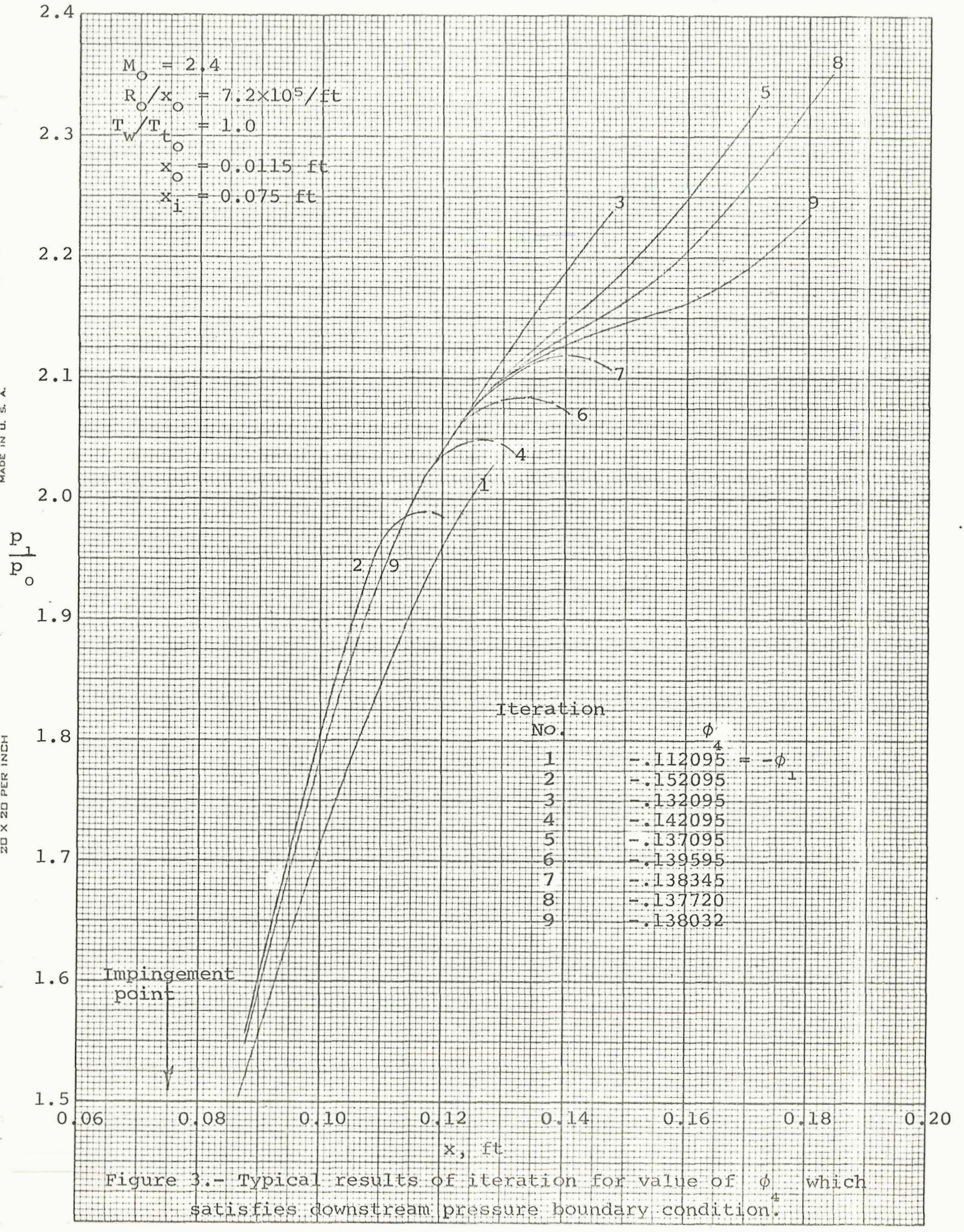

Figure 3.- Typical results of iteration for value of ϕ_4 which satisfies downstream pressure boundary condition.

CARD NO. 1

Variable	R_o/ℓ	M_o	γ	T_w/T_{t_o}
Card Col.	3	15	27	39
Format	X.XXXXE±YY	X.XXXXE±YY	X.XXXXE±YY	X.XXXXE±YY
Value				

CARD NO. 2

Variable	x_o	x_i	Δx_{PRINT}	NOUT
Card Col.	3	15	27	39
Format	X.XXXXE±YY	X.XXXXE±YY	X.XXXXE±YY	X
Value				

CARD NO. 3

Variable	PHITOL	PHHI	PHLO
Card Col.	3	14	29
Format	X.XXXXE±YY	-X.XXXXXXXE±YY	-X.XXXXXXXE±YY
Value			

Figure 4.- Format of input data to computer program.

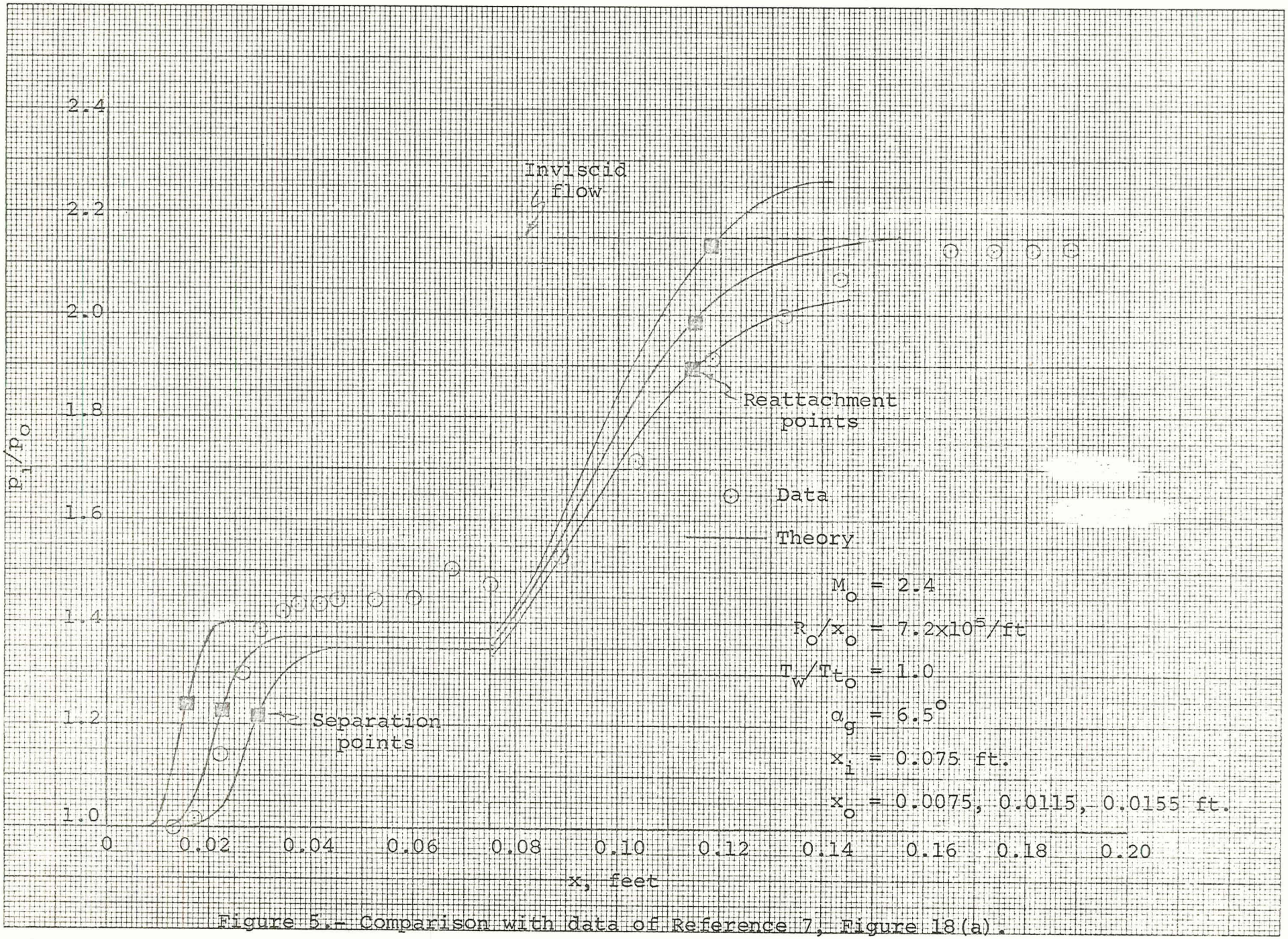

Figure 5.- Comparison with data of Reference 7, Figure 18(a).

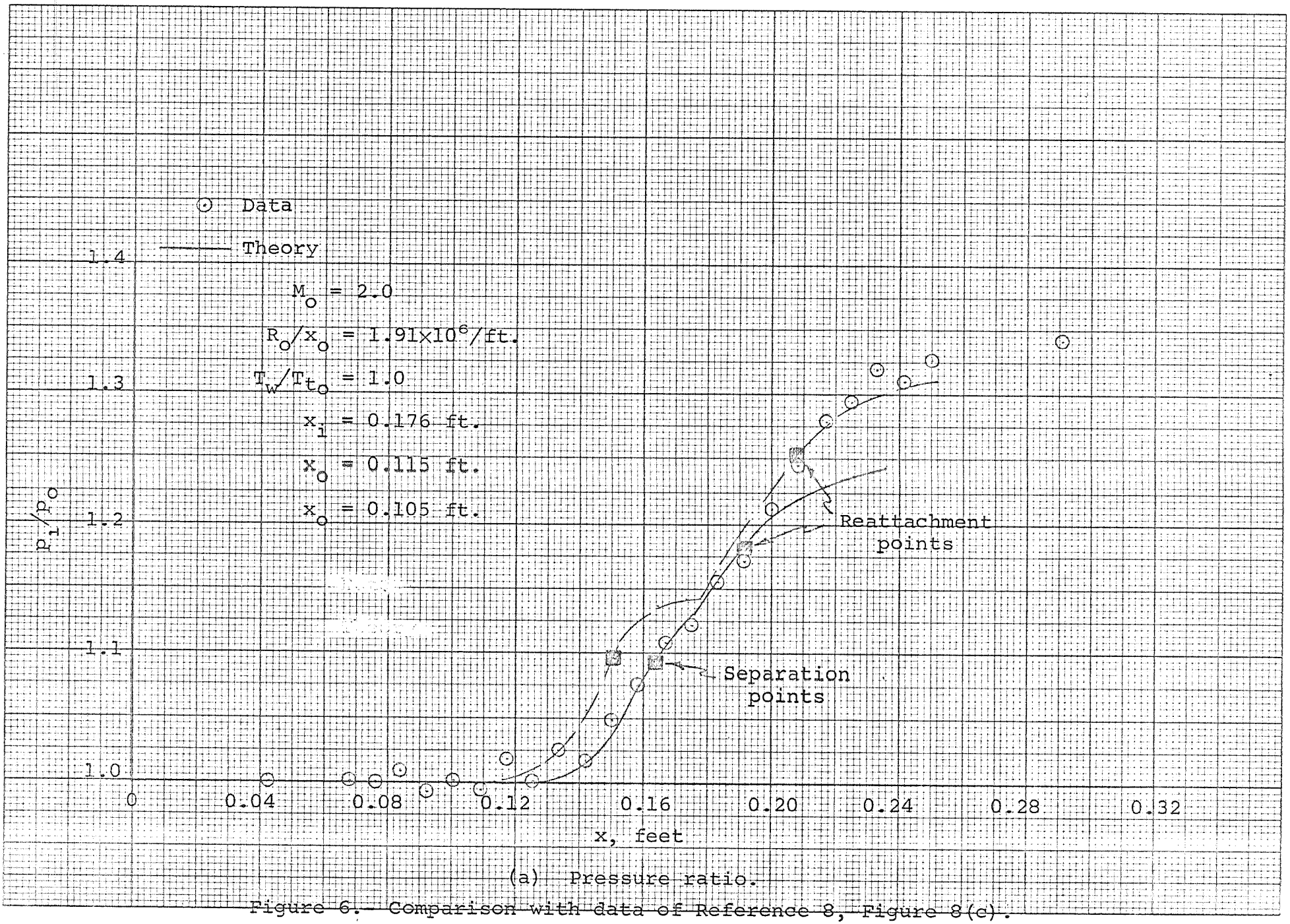

(a) Pressure ratio.

Figure 6.— Comparison with data of Reference 8, Figure 8(c).

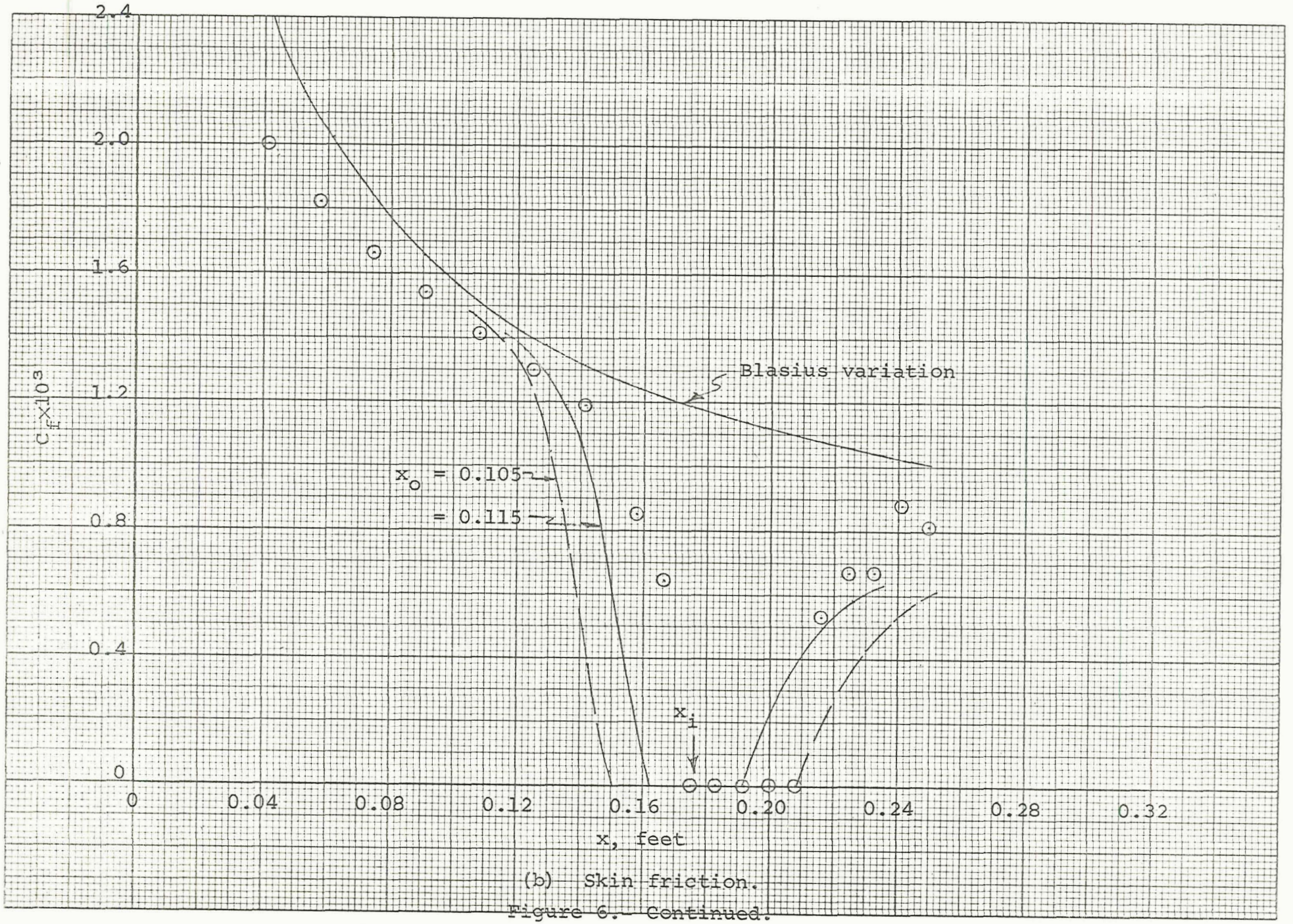

(b) Skin friction.

Figure 6.- Continued.

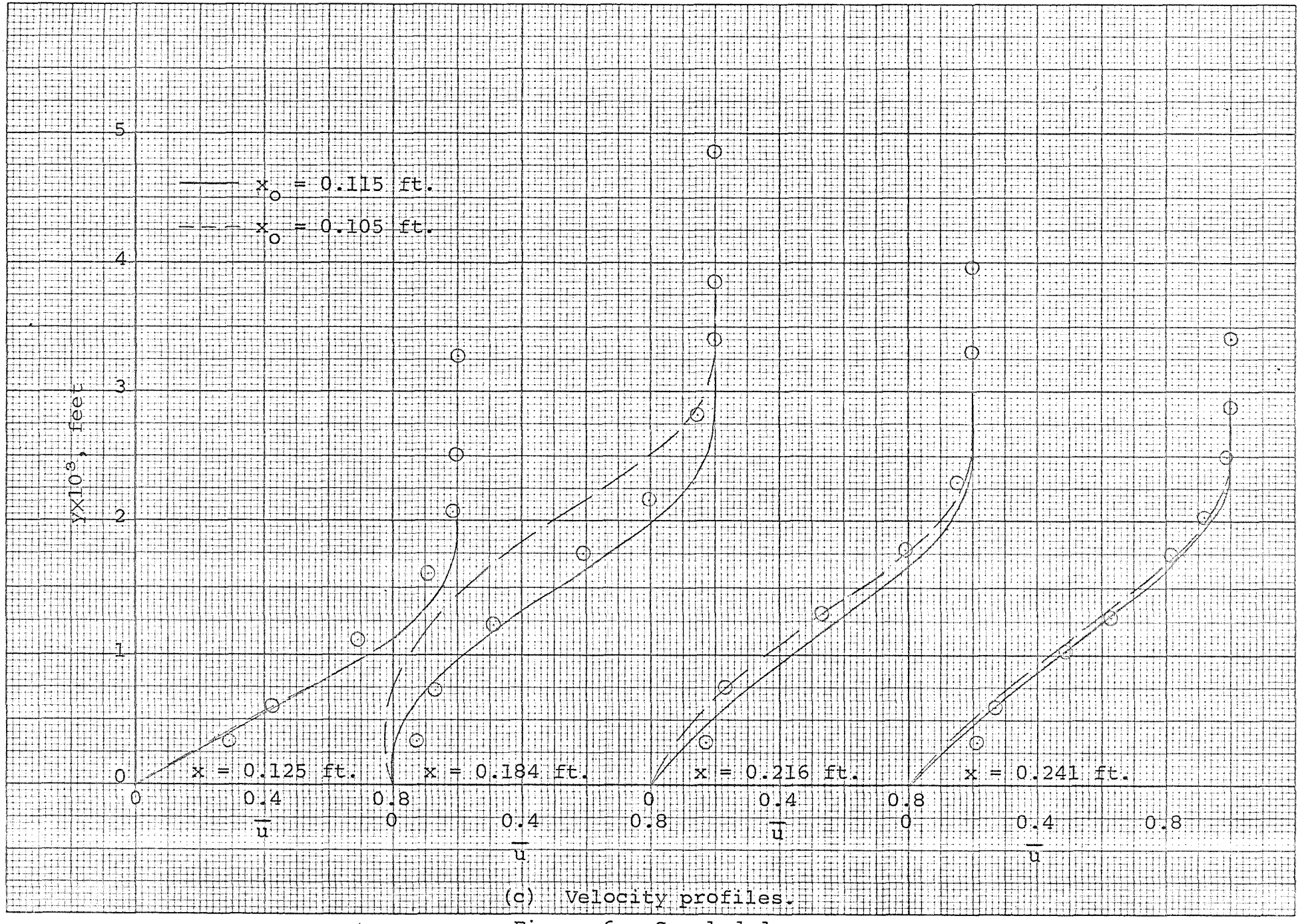

(c) Velocity profiles.

Figure 6.- Concluded.

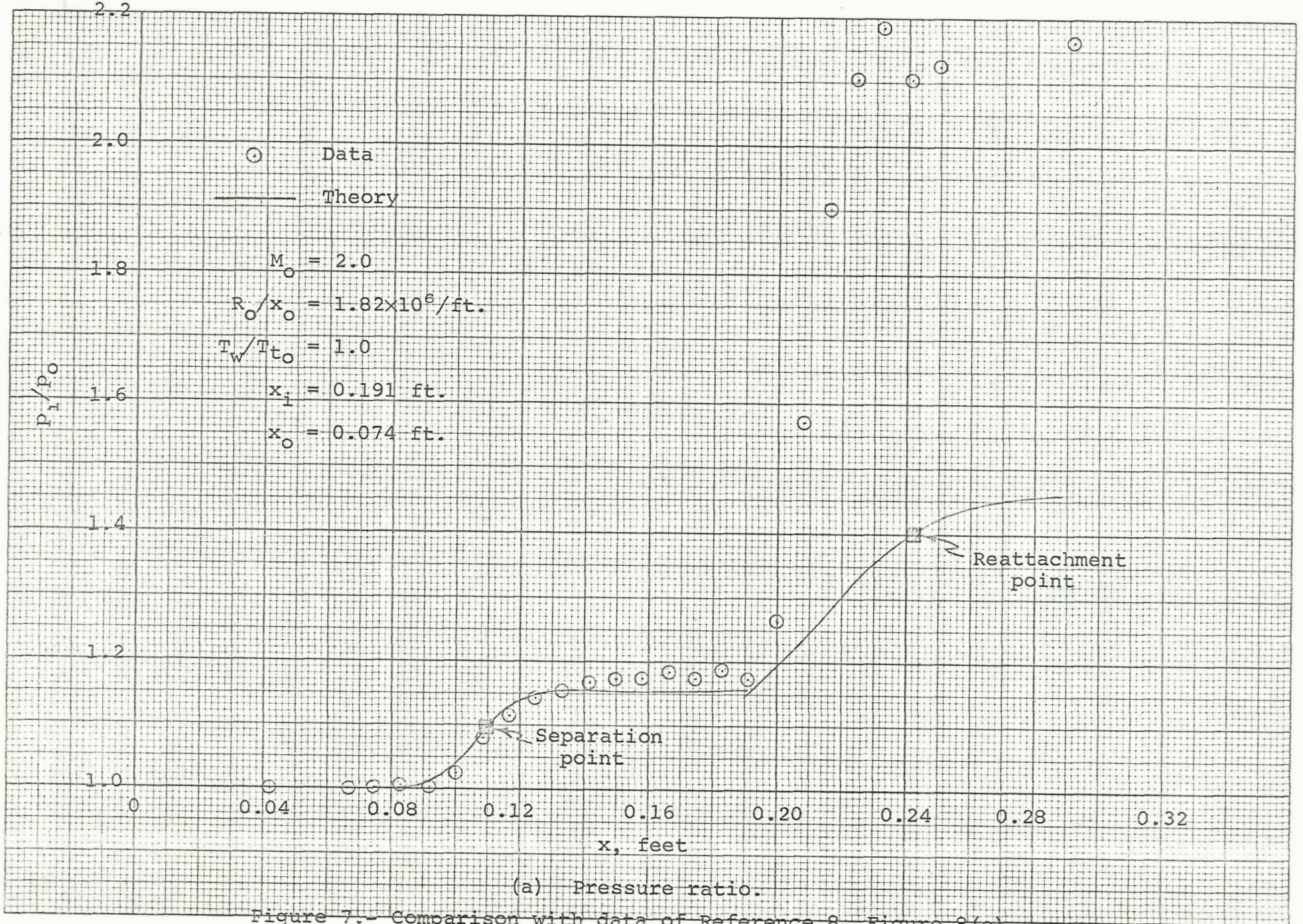

(a) Pressure ratio.

Figure 7.- Comparison with data of Reference 8, Figure 8(e).

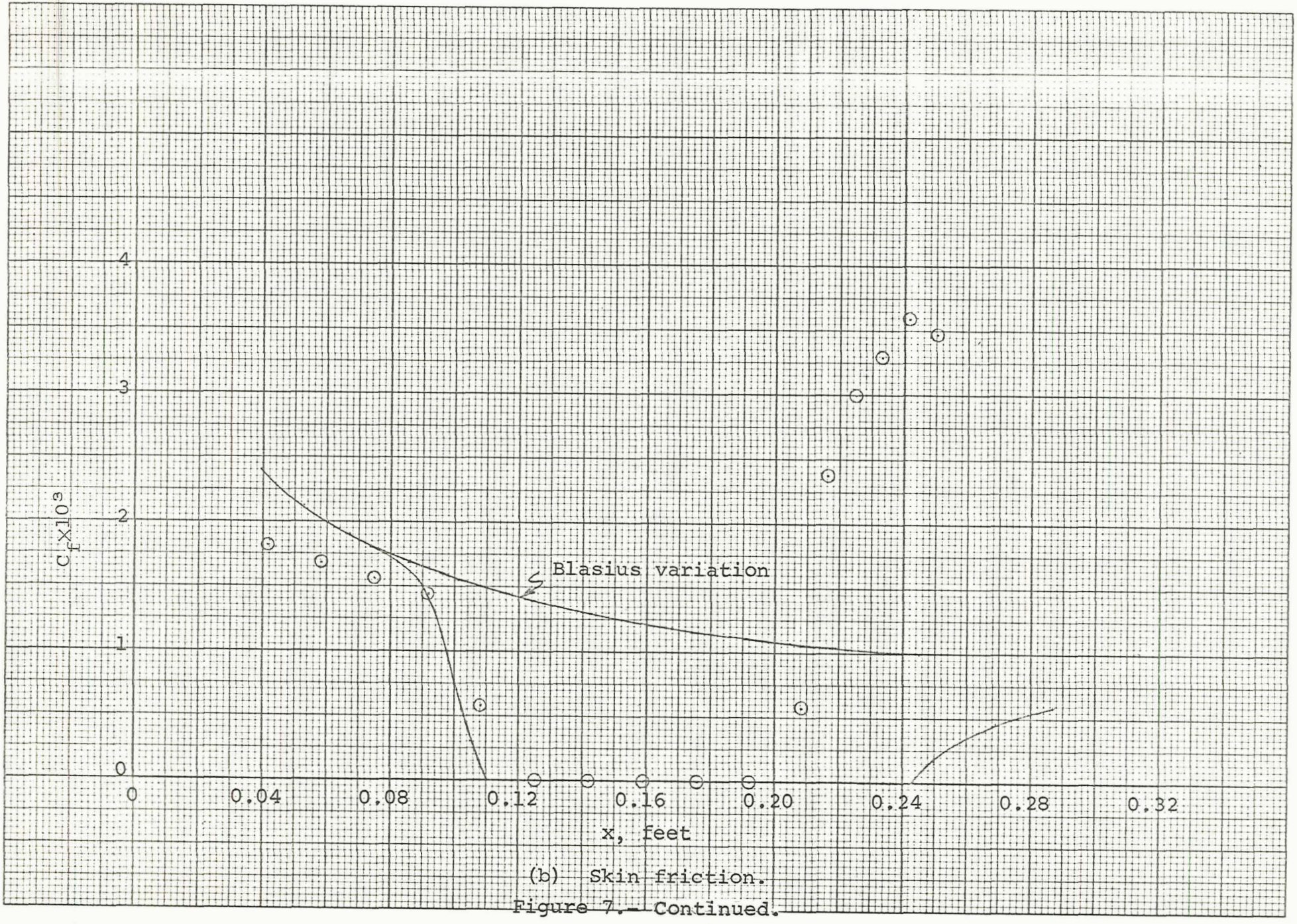

(b) Skin friction.

Figure 7.- Continued.

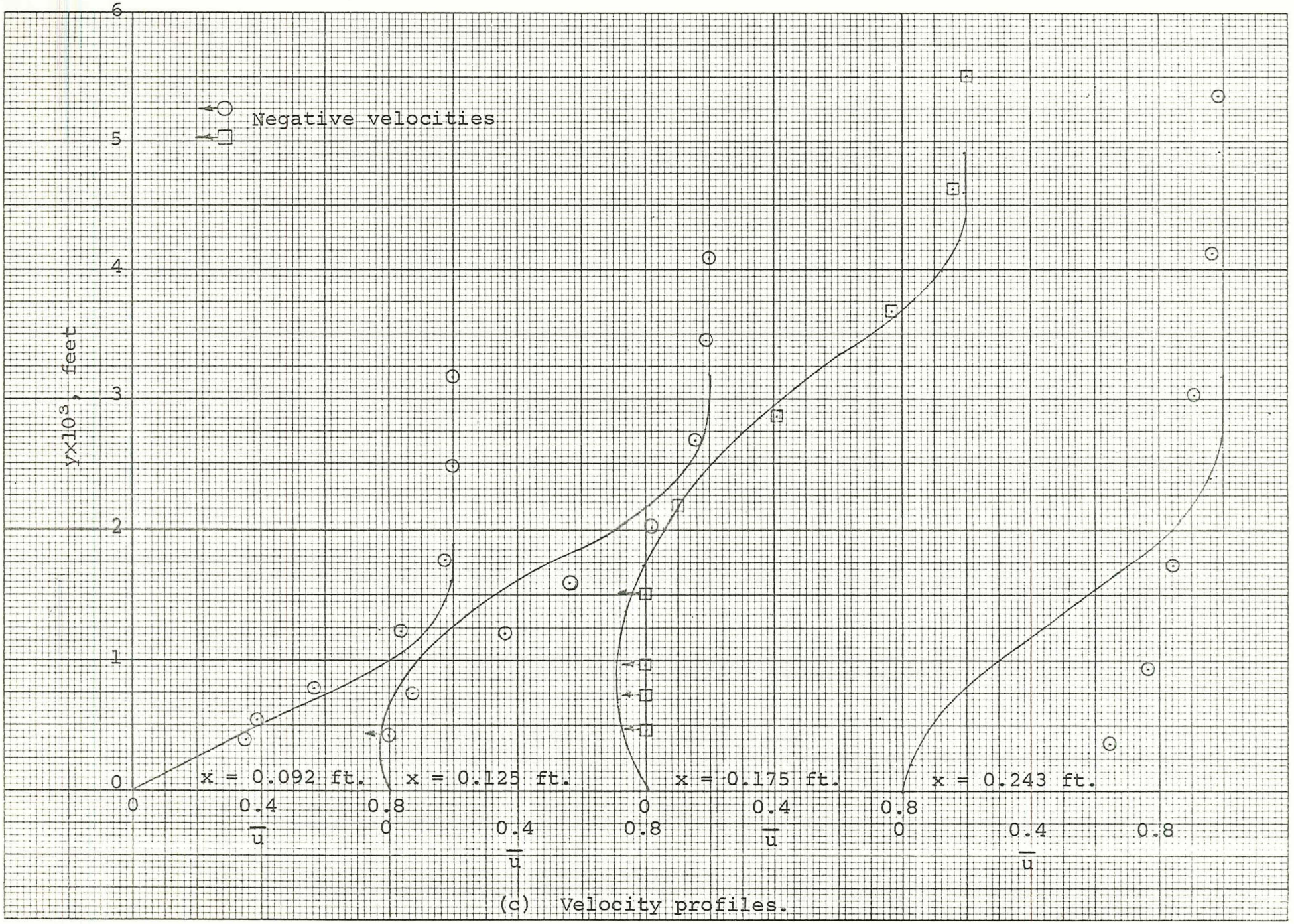

(c) Velocity profiles.

Figure 7.- Concluded.

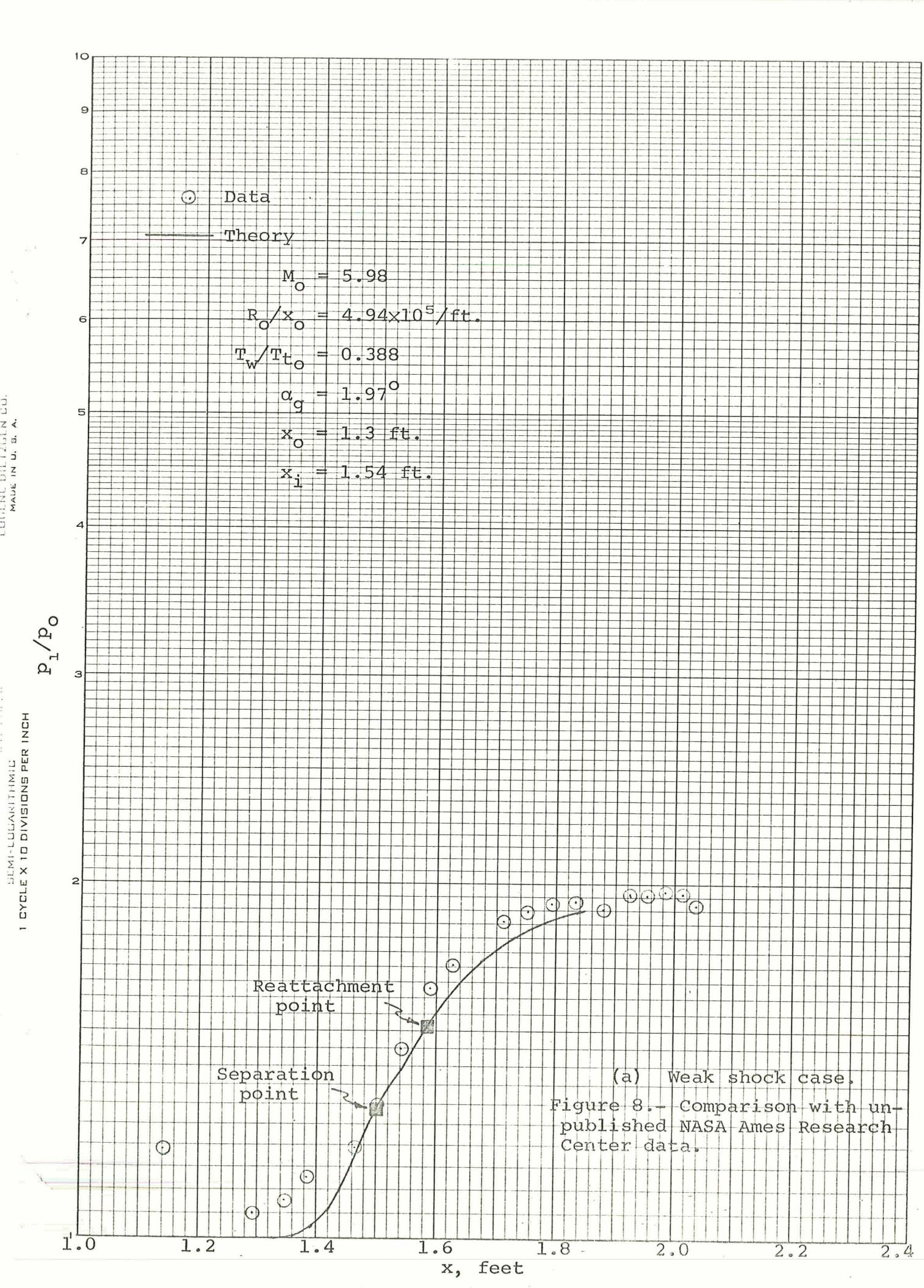

(a) Weak shock case.

Figure 8.- Comparison with unpublished NASA Ames Research Center data.

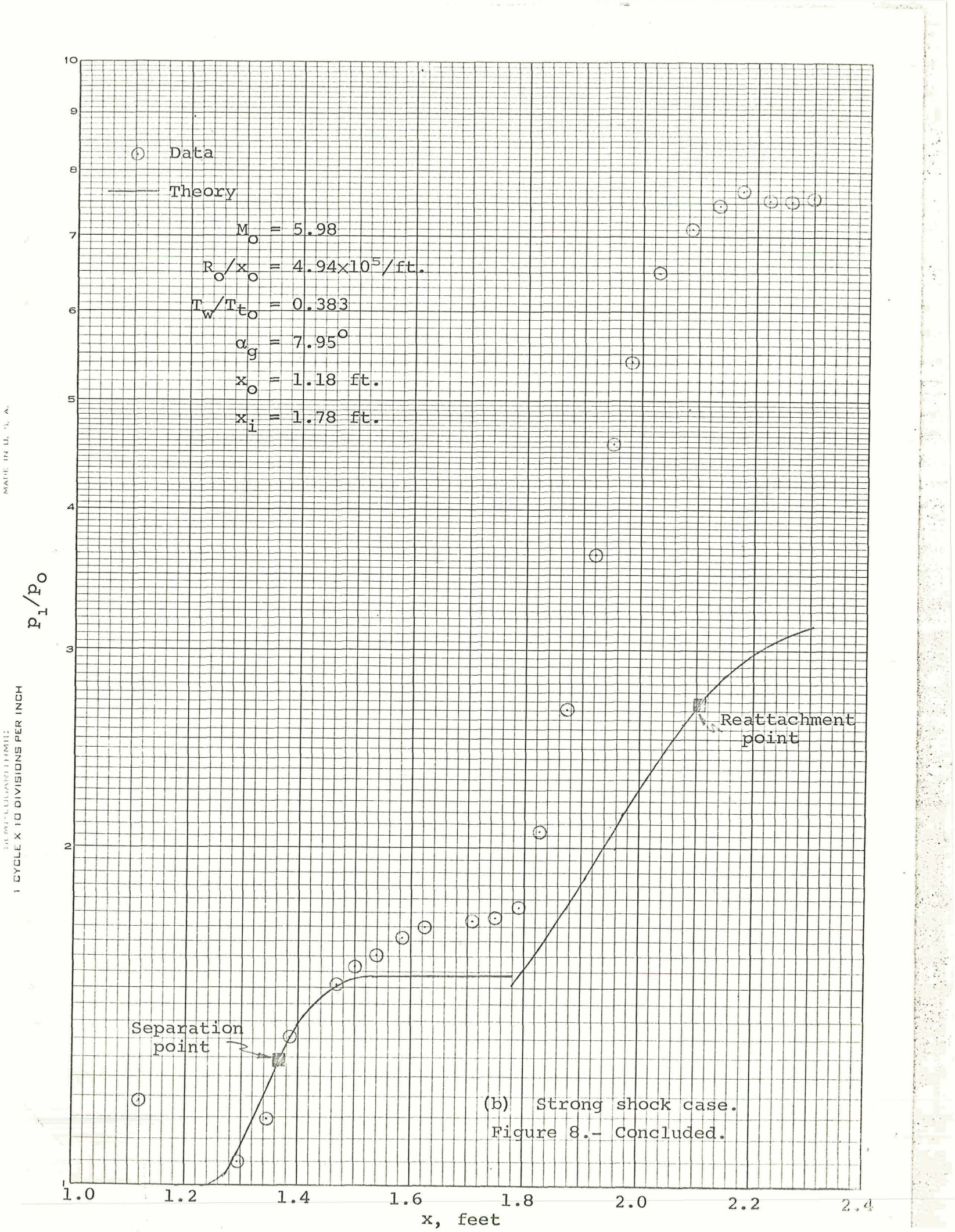

(b) Strong shock case.

Figure 8.- Concluded.

APPENDIX A

DIFFERENTIAL EQUATIONS FOR ATTACHED FLOW REGIONS

The differential equations which are solved in the attached flow regions are presented in this appendix without derivation. The four momentum equations are

$$g_1\dot{c}_0 + g_2\dot{c}_1 + g_3\dot{c}_2 + d_1\dot{c}_3 + \left[\left(\overline{f}_1 + \overline{f}_2\right) + \overline{H}_1 - E_0\overline{N}_0\right]\frac{\dot{U}_1}{U_1} = \frac{\sqrt{c_3}}{c_0} \tag{A-1}$$

$$g_2\dot{c}_0 + g_3\dot{c}_1 + g_4\dot{c}_2 + d_2\dot{c}_3 + \left[-\left(\overline{f}_1 - \overline{f}_2 - 2\overline{f}_3\right) - \left(\overline{H}_1 - 2\overline{H}_2\right) + E_0\left(\overline{N}_0 - 2\overline{N}_1\right)\right]\frac{\dot{U}_1}{U_1} = 2(P_0 - P_1) - \frac{\sqrt{c_3}}{c_0} \tag{A-2}$$

$$g_3\dot{c}_0 + g_4\dot{c}_1 + g_5\dot{c}_2 + d_3\dot{c}_3 + \left[-\left(2\overline{f}_2 - \overline{f}_3 - 3\overline{f}_4\right) - \left(2\overline{H}_2 - 3\overline{H}_3\right) + E_0\left(2\overline{N}_1 - 3\overline{N}_2\right)\right]\frac{\dot{U}_1}{U_1} = -2\left[(P_0 - P_1) - 3(P_1 - P_2)\right] \tag{A-3}$$

$$g_4\dot{c}_0 + g_5\dot{c}_1 + g_6\dot{c}_2 + d_4\dot{c}_3 + \left[-\left(3\overline{f}_3 - \overline{f}_4 - 4\overline{f}_5\right) - \left(3\overline{H}_3 - 4\overline{H}_4\right) + E_0\left(3\overline{N}_2 - 4\overline{N}_3\right)\right]\frac{\dot{U}_1}{U_1} = -6\left[(P_1 - P_2) - 2(P_2 - P_3)\right] \tag{A-4}$$

The free interaction equation is

$$\left[\left(S_w + 1 + E_0\sqrt{c_3}\right)g_0 - E_0\right]\dot{c}_0 + \left[\left(S_w + 1 + E_0\sqrt{c_3}\right)g_1 - \frac{E_0}{2}\right]\dot{c}_1 + \left[\left(S_w + 1 + E_0\sqrt{c_3}\right)g_2 - \frac{E_0}{3}\right]\dot{c}_2 + \left[\left(S_w + 1 + E_0\sqrt{c_3}\right)d_0 + \frac{E_0\overline{f}_1}{2\sqrt{c_3}}\right]\dot{c}_3 + p_2\left[(p_7 - 1)\left(\overline{H}_1 - E_0\overline{N}_0 + \overline{f}_1\right) + (p_8 - 1)\overline{f}_2\right]\frac{\dot{U}_1}{U_1} + \left(\overline{f}_1\sqrt{c_3} - \overline{N}_0\right)\dot{E}_0 = \frac{\sqrt{R_0}}{1 + m_0}\tan\phi_1 - p_2\frac{\sqrt{c_3}}{c_0} \tag{A-5}$$

and the energy equation is

$$- \frac{E_o}{6}\dot{c}_o - \frac{E_o}{12}\dot{c}_1 - \frac{E_o}{20}\dot{c}_2 + \frac{E_o}{2\sqrt{c_3}}\left(\overline{f}_2 - \overline{f}_3\right)\dot{c}_3 + \left\{ - \left(S_w + E_o\sqrt{c_3}\right)\left(\overline{H}_1 - \overline{H}_2\right) \right.$$

$$\left. - \left(\overline{H}_1 - \overline{H}_3\right) + E_o^2\left[\left(\overline{f}_2 - \overline{f}_3\right) + c_3\left(\overline{f}_1 - \overline{f}_2\right)\right] - E_o\left(\overline{N}_o - \overline{N}_2\right)\right\}\frac{\dot{U}_1}{U_1}$$

$$+ \left[\sqrt{c_3}\left(\overline{f}_2 - \overline{f}_3\right) - \left(\overline{N}_1 - \overline{N}_2\right)\right]\dot{E}_o$$

$$= E_o\left[\frac{1}{2c_o}\left(1 - 4c_3\right) + \left(Q_o - Q_1\right)\left(2c_3 - 1\right) + 3\left(Q_1 - Q_2\right)\right] \qquad \text{(A-6)}$$

The following notation has been used in specifying the coefficients

$$d_n = c_o\dot{g}_n + c_1\dot{g}_{n+1} + c_2\dot{g}_{n+2} \qquad \text{(A-7)}$$

$$\overline{f}_n = c_o g_{n-1} + c_1 g_n + c_2 g_{n+1} \qquad \text{(A-8)}$$

$$g_n = \int_o^1 \frac{\overline{u}^n}{\sqrt{\overline{u} + c_3}}\, d\overline{u} \qquad \text{(A-9)}$$

$$\dot{g}_n = \frac{dg_n}{dc_3} = -\frac{1}{2}\int_o^1 \frac{\overline{u}^n}{\left(\overline{u} + c_3\right)^{3/2}}\, d\overline{u} \qquad \text{(A-10)}$$

$$\overline{H}_n = \left(S_w + E_o\sqrt{c_3}\right)\overline{f}_n \qquad \text{(A-11)}$$

$$\overline{N}_n = \frac{c_o}{n+1} + \frac{c_1}{n+2} + \frac{c_2}{n+3} \qquad \text{(A-12)}$$

$$
\left.
\begin{aligned}
p_2 &= \frac{m_1}{1 + m_1} \\
p_3 &= \frac{3\gamma - 1}{\gamma - 1} - \frac{1 + m_1}{m_1} \\
p_4 &= 1 + \frac{m_1}{1 + m_1}\left(\frac{\gamma + 1}{\gamma - 1}\right) \\
p_5 &= 1 + p_2 p_6 \\
p_6 &= \frac{\sqrt{M_1^2 - 1}}{m_1} \tan \phi_1 \\
p_7 &= \frac{p_3 - p_6}{p_5} \\
p_8 &= \frac{p_4 - p_2 p_6}{p_5}
\end{aligned}
\right\} \qquad \text{(A-13)}
$$

$$
P_n = \int_0^1 \frac{\bar{u}^n \sqrt{\bar{u} + c_3}}{c_0 + c_1 \bar{u} + c_2 \bar{u}^2} \, d\bar{u} \qquad \text{(A-14)}
$$

$$
Q_n = \int_0^1 \frac{\bar{u}^n}{c_0 + c_1 \bar{u} + c_2 \bar{u}^2} \, d\bar{u} \qquad \text{(A-15)}
$$

APPENDIX B

DIFFERENTIAL EQUATIONS FOR SEPARATED FLOW REGION

The differential equations which are solved in the separated flow region are presented in this appendix without derivation. The four momentum equations are

$$\left(g_1 + \frac{\eta_s^2 \alpha_s}{6c_o}\right)\dot{c}_o + g_2\dot{c}_1 + g_3\dot{c}_2 + \left(d_1 - \frac{\eta_s^2}{12c_o\sqrt{c_3}}\right)\dot{c}_3 + \left[\left(\overline{f}_1 + \overline{f}_2\right) + \tilde{H}_1 - E_o\overline{N}_o\right]\frac{\dot{U}_1}{U_1} - \frac{\eta_s\alpha_s}{3}\dot{\eta}_s = \frac{\sqrt{c_3}}{c_o} \tag{B-1}$$

$$g_2\dot{c}_o + g_3\dot{c}_1 + g_4\dot{c}_2 + d_2\dot{c}_3 + \left[-\left(\overline{f}_1 - \overline{f}_2 - 2\overline{f}_3\right) - \left(\tilde{H}_1 - 2\tilde{H}_2\right) + E_o\left(\overline{N}_o - 2\overline{N}_1\right)\right]\frac{\dot{U}_1}{U_1} = 2(P_o - P_1) - \frac{\sqrt{c_3}}{c_o} \tag{B-2}$$

$$g_3\dot{c}_o + g_4\dot{c}_1 + g_5\dot{c}_2 + d_3\dot{c}_3 + \left[-\left(2\overline{f}_2 - \overline{f}_3 - 3\overline{f}_4\right) - \left(2\tilde{H}_2 - 3\tilde{H}_3\right) + E_o\left(2\overline{N}_1 - 3\overline{N}_2\right)\right]\frac{\dot{U}_1}{U_1} = -2\left[(P_o - P_1) - 3(P_1 - P_2)\right] \tag{B-3}$$

$$g_4\dot{c}_o + g_5\dot{c}_1 + g_6\dot{c}_2 + d_4\dot{c}_3 + \left[-\left(3\overline{f}_3 - \overline{f}_4 - 4\overline{f}_5\right) - \left(3\tilde{H}_3 - 4\tilde{H}_4\right) + E_o\left(3\overline{N}_2 - 4\overline{N}_3\right)\right]\frac{\dot{U}_1}{U_1} = -6\left[(P_1 - P_2) - 2(P_2 - P_3)\right] \tag{B-4}$$

The free-interaction equation is

$$\left[\left(S_s + 1 + E_o\sqrt{c_3}\right) g_o - E_o - \frac{\eta_s^2\alpha_s}{6c_o} + p_2\,\frac{\eta_s^3\alpha_s^2}{15c_o}\right]\dot{c}_o$$

$$+\left[\left(S_s + 1 + E_o\sqrt{c_3}\right) g_1 - \frac{E_o}{2}\right]\dot{c}_1 + \left[\left(S_s + 1 + E_o\sqrt{c_3}\right) g_2 - \frac{E_o}{3}\right]\dot{c}_2$$

$$+\left[\left(S_s + 1 + E_o\sqrt{c_3}\right) d_o + \frac{E_o\overline{f}_1}{2\sqrt{c_3}} + \frac{\eta_s^2}{12c_o\sqrt{c_3}} - p_2\,\frac{\eta_s^3}{30c_o^2}\right]\dot{c}_3$$

$$+ p_2\left\{(p_7 - 1)\left(\tilde{H}_1 - E_o\overline{N}_o + \overline{f}_1\right) + p_7\left[\eta_s\left(1 + \frac{S_s + S_w}{2}\right) + \frac{\eta_s^2\alpha_s}{6}\right]\right.$$

$$\left. + (p_8 - 1)\overline{f}_2 - p_8\left(\frac{\eta_s^2\alpha_s}{6} + \frac{\eta_s^3\alpha_s^2}{30}\right)\right\}\frac{\dot{U}_1}{U_1} + \left(\overline{f}_1\sqrt{c_3} - \overline{N}_o\right)\dot{E}_o$$

$$+\left(1 + \frac{S_s + S_w}{2} + \frac{\eta_s\alpha_s}{3} - p_2\,\frac{\eta_s^2\alpha_s^2}{10}\right)\dot{\eta}_s + \left(\overline{f}_1 + \frac{\eta_s}{2}\right)\dot{S}_s$$

$$= \frac{\sqrt{R_o}}{1 + m_o}\tan\phi_1 - p_2\,\frac{\sqrt{c_3}}{c_o} \qquad \text{(B-5)}$$

and the energy equation is

$$-\left(\frac{E_o}{6} + \frac{E_o\eta_s^2\alpha_s^2}{6}\right)\dot{c}_o - \frac{E_o}{12}\,\dot{c}_1 - \frac{E_o}{20}\,\dot{c}_2 + \left[\frac{E_o}{2\sqrt{c_3}}\left(\overline{f}_2 - \overline{f}_3\right) + \frac{E_o\eta_s^2}{12c_o}\right]\dot{c}_3$$

$$+\left\{-\left(S_s + E_o\sqrt{c_3}\right)\left(\tilde{H}_1 - \tilde{H}_2\right) - \left(\tilde{H}_1 - \tilde{H}_3\right) + E_o^2\left[\left(\overline{f}_2 - \overline{f}_3\right) + c_3\left(\overline{f}_1 - \overline{f}_2\right)\right]\right.$$

$$\left. - E_o\left(\overline{N}_o - \overline{N}_2\right)\right\}\frac{\dot{U}_1}{U_1} + \left[\sqrt{c_3}\left(\overline{f}_2 - \overline{f}_3\right) - \left(\overline{N}_1 - \overline{N}_2\right)\right]\dot{E}_o$$

$$+\frac{E_o\sqrt{c_3}\eta_s\alpha_s}{3}\,\dot{\eta}_s + \left(\overline{f}_2 - \overline{f}_3\right)\dot{S}_s$$

$$= E_o\left[\frac{1}{2c_o}\left(1 - 4c_3\right) + \left(Q_o - Q_1\right)\left(2c_3 - 1\right) + 3\left(Q_1 - Q_2\right)\right]$$

$$\text{(B-6)}$$

The match of the first derivatives of velocity profiles (Eq. (49)), after differentiation with respect to ξ, is

$$-\frac{\sqrt{c_3}}{c_0^2}\dot{c}_0 + \frac{1}{2c_0\sqrt{c_3}}\dot{c}_3 = \dot{\alpha}_s \tag{B-7}$$

The match of the second derivatives of the velocity profile (Eq. (50)) yields

$$\frac{1}{c_0}\left\{\eta_s\left[\alpha_s^2\left(1+\frac{3c_1}{2c_0}\right)-\frac{1}{2c_0^2}\right]+\alpha_s\right\}\dot{c}_0 - \frac{\eta_s\alpha_s^2}{2c_0}\dot{c}_1$$
$$-\frac{1}{2c_0\sqrt{c_3}}\left[\eta_s\alpha_s\left(1+\frac{c_1}{c_0}\right)+1\right]\dot{c}_3$$
$$=\left[\frac{\alpha_s^2}{2}\left(1+\frac{c_1}{c_0}\right)-\frac{1}{4c_0^2}\right]\dot{\eta}_s \tag{B-8}$$

and the match of the first derivatives of the temperature profiles (Eq. (51)) becomes

$$\frac{\eta_s\alpha_s}{c_0}\left(S_s+\frac{E_0}{2\sqrt{c_3}}\right)\dot{c}_0 - \frac{S_s\eta_s}{2c_0\sqrt{c_3}}\dot{c}_3 - \frac{\eta_s}{2c_0}\dot{E}_0 - \alpha_s\left(S_s+\frac{E_0}{2\sqrt{c_3}}\right)\dot{\eta}_s$$
$$=\left(1+\eta_s\alpha_s\right)\dot{S}_s \tag{B-9}$$

The notation used in the coefficients is that given by Equations (A-7) through (A-15) of Appendix A and the additional quantity

$$\tilde{H}_n = \left(S_s + E_0\sqrt{c_3}\right)\overline{f}_n \tag{B-10}$$

In the constant pressure region the free interaction equation, Equation (B-5), is not used and the $\dot{U}_1$ terms in the other equations are set equal to zero.